Weakly Coupled Molecular Photonic Wires: Synthesis and Excited-State Energy-Transfer Dynamics

Arounaguiry Ambroise,[†] Christine Kirmaier,[‡] Richard W. Wagner,[†] Robert S. Loewe,[†] David F. Bocian,*[,§] Dewey Holten,*[,‡] and Jonathan S. Lindsey*[,†]

Department of Chemistry, North Carolina State University, Raleigh, North Carolina 27695-8204, Department of Chemistry, Washington University, St. Louis, Missouri 63130-4889, and Department of Chemistry, University of California, Riverside, California 92521-0403

jlindsey@ncsu.edu

Received January 28, 2002

Molecular photonic wires, which absorb light and undergo excited-state energy transfer, are of interest as biomimetic models for photosynthetic light-harvesting systems and as molecular devices with potential applications in materials chemistry. We describe the stepwise synthesis of four molecular photonic wires. Each wire consists of an input unit, transmission element, and output unit. The input unit consists of a boron-dipyrrin dye or a perylene-monoimide dye (linked either at the *N*-imide or the C9 position); the transmission element consists of one or three zinc porphyrins affording short or long wires, respectively; and the output unit consists of a free base (Fb) porphyrin. The components in the arrays are joined in a linear architecture via diarylethyne linkers (an ethynylphenyl linker is attached to the C9-linked perylene). The wires have been examined by static absorption, static fluorescence, and time-resolved absorption spectroscopy. Each wire (with the exception of the C9-linked perylene wire) exhibits a visible absorption spectrum that is the sum of the spectra of the component parts, indicating the relatively weak electronic coupling between the components. Excitation of each wire at the wavelength where the input unit absorbs preferentially (typically 480−520 nm) results in emission almost exclusively from the Fb porphyrin. The static emission and time-resolved data indicate that the overall rate constants and quantum efficiencies for end-to-end (i.e., input to output) energy transfer are as follows: perylene-(*N*-imide)-linked short wire, $(33\ ps)^{-1}$ and >99%; perylene-(C9)-linked short wire, $(26\ ps)^{-1}$ and >99%; boron-dipyrrin-based long wire, $(190\ ps)^{-1}$ and 81%; perylene-(*N*-imide)-linked long wire, $(175\ ps)^{-1}$ and 86%. Collectively, the studies provide valuable insight into the singlet−singlet excited-state energy-transfer properties in weakly coupled molecular photonic wires.

Introduction

About eight years ago, we described the design and static spectroscopic properties of a molecular photonic wire (**1**) (Chart 1).[1] The inspiration for this work came from the photosynthetic light-harvesting arrays, wherein efficient energy transfer occurs among large numbers of porphyrinic pigments.[2] The motivation for the preparation and study of **1** was to explore analogous energy-transfer processes in synthetic constructs that might have application in the field of materials chemistry.

The wire is composed of a boron-dipyrrin (BDPY) input unit, three zinc porphyrins, and a free base (Fb) porphyrin output unit joined via diarylethyne linkers. The visible absorption spectrum of **1** is essentially the sum of the spectra of the component parts, which is one of several indicators of the relatively weak electronic coupling between the constituents in the ground and lowest excited singlet states. Nevertheless, excitation at 483 nm, a wavelength at which most of the absorption stems from the BDPY unit, results in emission predominantly from the Fb porphyrin. The energy-transfer efficiency from end-to-end in the wire was estimated to be 76%.[1] These results showed that singlet−singlet excited-state energy transfer could be quite efficient in a collection of weakly coupled chromophores. The success of this work prompted the synthesis and characterization of a large number of other weakly coupled multiporphyrin arrays, including optoelectronic gates[3−5] and a variety of light-harvesting architectures.[6−9] We also prepared a number of dyads and

[†] North Carolina State University.
[‡] Washington University.
[§] University of California.

(1) Wagner, R. W.; Lindsey, J. S. *J. Am. Chem. Soc.* **1994**, *116*, 9759−9760.

(2) (a) Larkum, A. W. D.; Barrett, J. *Adv. Bot. Res.* **1983**, *10*, 1−219. (b) *Photosynthetic Light-Harvesting Systems*; Scheer, H., Siegried, S., Eds.; W. de Gruyter: Berlin, 1988. (c) Mauzerall, D. C.; Greenbaum, N. L. *Biochim. Biophys. Acta* **1989**, *974*, 119−140. (d) McDermott, G.; Prince, S. M.; Freer, A. A.; Hawethornthwaite-Lawless, A. M.; Papiz, M. Z.; Cogdell, R. J.; Isaacs, N. W. *Nature* **1995**, *374*, 517−521. (e) Karrasch, S.; Bullough, P. A.; Ghosh, R. *EMBO J.* **1995**, *14*, 631−638. (f) Pullerits, T.; Sundstrom, V. *Acc. Chem. Res.* **1996**, *29*, 381−389.

(3) Wagner, R. W.; Lindsey, J. S.; Seth, J.; Palaniappan, V.; Bocian, D. F. *J. Am. Chem. Soc.* **1996**, *118*, 3996−3997.

(4) Ambroise, A.; Wagner R. W.; Rao, P. D.; Riggs, J. A.; Hascoat, P.; Diers, J. G.; Seth, J.; Lammi, R. K.; Bocian, D. F.; Holten, D.; Lindsey, J. S. *Chem. Mater.* **2001**, *13*, 1023−1034.

(5) Lammi, R. K.; Wagner, R. W.; Ambroise, A.; Diers, J. R.; Bocian, D. F.; Holten, D.; Lindsey, J. S. *J. Phys. Chem. B* **2001**, *105*, 5341−5352.

(6) Li, F.; Gentemann, S.; Kalsbeck, W. A.; Seth, J.; Lindsey, J. S.; Holten, D.; Bocian, D. F. *J. Mater. Chem.* **1997**, *7*, 1245−1262.

(7) Li, F.; Yang, S. I.; Ciringh, Y.; Seth, J.; Martin, C. H., III; Singh, D. L.; Kim, D.; Birge, R. R.; Bocian, D. F.; Holten, D.; Lindsey, J. S. *J. Am. Chem. Soc.* **1998**, *120*, 10001−10017.

(8) (a) Li, J.; Ambroise, A.; Yang, S. I.; Diers, J. R.; Seth, J.; Wack, C. R.; Bocian, D. F.; Holten, D.; Lindsey, J. S. *J. Am. Chem. Soc.* **1999**, *121*, 8927−8940. (b) Ambroise, A.; Li, J.; Yu, L.; Lindsey, J. S. *Org. Lett.* **2000**, *2*, 2563−2566. (c) Yu, L.; Lindsey, J. S. *J. Org. Chem.* **2001**, *66*, 7402−7419.

10.1021/jo025561i CCC: $22.00
Published on Web 05/08/2002

Chart 1

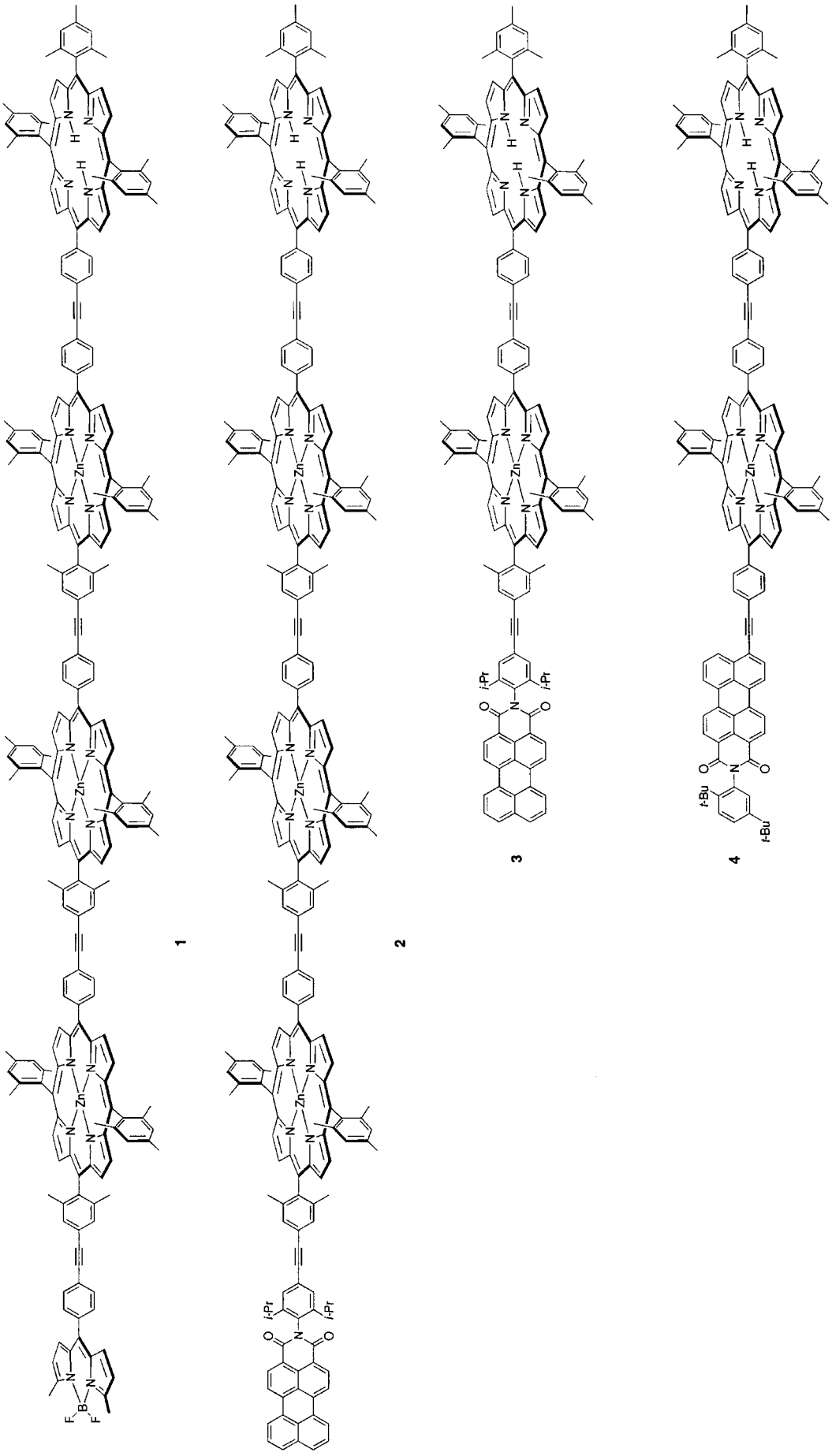

triads for probing the nature of electronic communication that underlies efficient excited-state energy transfer.[10] The results of these studies demonstrated that excited-state energy transfer in the diarylethyne-linked arrays occurs predominantly via a through-bond process, with only a minor through-space contribution.

A number of considerations led to the design of **1**, including the choice of substituents at the nonlinking positions of the porphyrins, the linkers joining the pigments, and the nature of the output and input units. The rationale for the molecular design was as follows:

(1) Mesityl groups were introduced at all nonlinking meso positions of the porphyrins as a means of suppressing cofacial aggregation, thereby increasing the solubility of the array.

(2) Diarylethyne linkers were chosen owing to (i) their relative rigidity,[11] (ii) their length, giving rise to an interporphyrin separation (center-to-center separation of ~20 Å) that should suppress competing through-space electron-transfer reactions, (iii) the absence of direct, extensive conjugation with the porphyrin macrocycle, and (iv) their compatibility with a synthetic building block approach.[12] Methyl groups were incorporated at sites on several of the linkers to engender increased solubility (as with the mesityl groups) and also because the presence of methyl groups greatly facilitated the isolation of a key porphyrin building block from the mixture of porphyrins obtained in a statistical synthesis.[12]

(3) The Fb porphyrin was chosen as the output unit because a Fb porphyrin has a lower energy excited state than does the corresponding Zn chelate, thereby enabling irreversible energy transfer between Zn and Fb porphyrins.

(4) The BDPY dye was chosen as an input unit because members of this class of dyes met a handful of key criteria for a suitable accessory pigment including[13] (i) absorption in the trough between the porphyrin B and Q bands, (ii) an excited-state lifetime of sufficient duration for energy transfer to occur (typically indicated by the presence of at least a modest fluorescence quantum yield), (iii) a nonpolar nature, thereby facilitating processing and chromatography, and (iv) compatibility with the modular building block approach.

Subsequent analysis of BDPY monomers such as **BDPY-TMS** revealed a modest fluorescence quantum yield ($\Phi_f = 0.058$),[7] which is less than that of many BDPY dyes but more than sufficient for use as an input unit (Chart 2). However, the photoexcited BDPY dye exhibits a biphasic lifetime ($\tau = 15$, 520 ps; $\chi = 0.26{:}0.74$) owing to the presence of two excited-state conformers.[7] The corresponding BDPY−Zn porphyrin dyad, **BDPY−Zn**, exhibits two energy-transfer rates associated with the two BDPY excited-state conformers ($k_{trans} = (2.0\text{ ps})^{-1}$ and $(17\text{ ps})^{-1}$). Although the energy-transfer process is efficient ($\Phi_{trans} = 0.98$), the existence of two BDPY excited-state conformers/lifetimes is unattractive for an input unit because this complicates kinetic analysis of the energy-transfer dynamics in the wire.

Chart 2

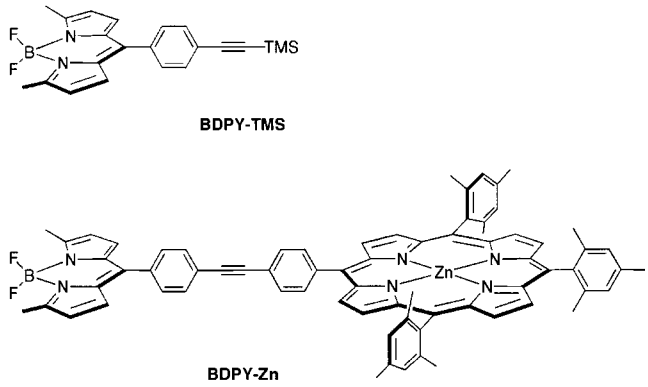

Although the BDPY dyes have many favorable qualities, their undesirable properties led us to prepare a number of dyads containing a perylene dye and a porphyrin.[14−18] Perylene-bis(imide) dyes typically have high fluorescence yields ($\Phi_f \sim 1.0$)[19,20] and relatively long-lived excited singlet states ($\tau = 3-5$ ns) with a monophasic lifetime.[21] These perylene-based dyes also absorb in the trough between the porphyrin B and Q bands,[22] are relatively nonpolar, and can be manipulated synthetically. The inclusion of one or more bulky substituents is essential for rendering perylene-based dyes soluble in organic solvents.[19−24] Most synthetic multichromophore model systems that incorporate perylene dyes have employed perylene-bis(imide) derivatives.[25] Dyads comprised of a porphyrin and a perylene-bis(imide) dye exhibit facile energy transfer from perylene to porphyrin. However, competing charge-transfer reactions (hole transfer from photoexcited perylene to the porphyrin and electron transfer from photoexcited porphyrin to the perylene) also occur in both polar and nonpolar solvents.[15] To suppress these reactions (at least in nonpolar media), we turned to the use of perylene-monoimide dyes, which are poorer electron acceptors.[14,17] Only a few synthetic

(9) del Rosario Benites, M.; Johnson, T. E.; Weghorn, S.; Yu, L.; Rao, P. D.; Diers, J. R.; Yang, S. I.; Kirmaier, C.; Bocian, D. F.; Holten, D.; Lindsey, J. S. *J. Mater. Chem.* **2002**, *12*, 65−80.

(10) Holten, D.; Bocian, D. F.; Lindsey, J. S. *Acc. Chem. Res.* **2002**, *35*, 57−69.

(11) Bothner-By, A. A.; Dadok, J.; Johnson, T. E.; Lindsey, J. S. *J. Phys. Chem.* **1996**, *100*, 17551−17557.

(12) Wagner, R. W.; Johnson, T. E.; Lindsey, J. S. *J. Am. Chem. Soc.* **1996**, *118*, 11166−11180.

(13) (a) Wagner, R. W.; Lindsey, J. S. *Pure Appl. Chem.* **1996**, *68*, 1373−1380. (b) Wagner, R. W.; Lindsey, J. S. *Pure Appl. Chem.* **1998**, *70 (8)*, p. i.

(14) Miller, M. A.; Lammi, R. K.; Prathapan, S.; Holten, D.; Lindsey, J. S. *J. Org. Chem.* **2000**, *65*, 6634−6649.

(15) Prathapan, S.; Yang, S. I.; Miller, M. A.; Bocian, D. F.; Holten, D.; Lindsey, J. S. *J. Phys. Chem. B* **2001**, *105*, 8237−8248.

(16) Yang, S. I.; Prathapan, S.; Miller, M. A.; Seth, J.; Bocian, D. F.; Lindsey, J. S.; Holten, D. *J. Phys. Chem. B* **2001**, *105*, 8249−8258.

(17) Yang, S. I.; Lammi, R. K.; Prathapan, S.; Miller, M. A.; Seth, J.; Diers, J. A.; Bocian, D. F.; Lindsey, J. S.; Holten, D. *J. Mater. Chem.* **2001**, *11*, 2420−2430.

(18) Loewe, R. S.; Tomizaki, K.; Chevalier, F.; Kirmaier, C.; Schwartz, J. K.; Diers, J. R.; Bocian, D. F.; Holten, D.; Lindsey, J. S. Manuscript in preparation.

(19) (a) Rademacher, A.; Märkle, S.; Langhals, H. *Chem. Ber.* **1982**, *115*, 2927−2934. (b) Ebeid, E. M.; El-Daly, S. A.; Langhals, H. *J. Phys. Chem.* **1988**, *92*, 4565−4568.

(20) Langhals, H. *Chem. Ber.* **1985**, *118*, 4641−4645.

(21) Ford, W. E.; Kamat, P. V. J. *Phys. Chem.* **1987**, *91*, 6373−6380.

(22) Demmig, S.; Langhals, H. *Chem. Ber.* **1988**, *121*, 225−230.

(23) Feiler, L.; Langhals, H.; Polborn, K. *Liebigs Ann.* **1995**, 1229−1244.

(24) Cormier, R. A.; Gregg, B. A. *Chem. Mater.* **1998**, *10*, 1309−1319.

(25) (a) Kaiser, H.; Lindner, J.; Langhals, H. *Chem. Ber.* **1991**, *124*, 529−535. (b) O'Neil, M. P.; Niemczyk, M. P.; Svec, W. A.; Gosztola, D.; Gaines, G. L., III; Wasielewski, M. R. *Science* **1992**, *257*, 63−65. (c) Wasielewski, M. R.; Gosztola, D.; Svec, W. A. *Mol. Cryst. Liq. Cryst.* **1994**, *253*, 289−296. (d) Langhals, H.; Gold, J. *J. Prakt. Chem.* **1996**, *338*, 654−659. (e) Langhals, H.; Jona, W. *Angew. Chem., Int. Ed. Engl.* **1998**, *37*, 952−955. (f) Langhals, H.; Gold, J. *Liebigs Ann./Recueil* **1997**, 1151−1153. (g) Kalinin, S.; Speckbacher, M.; Langhals, H.; Johannson, L. B.-Å. *Phys. Chem. Chem. Phys.* **2001**, *3*, 172−174.

Chart 3

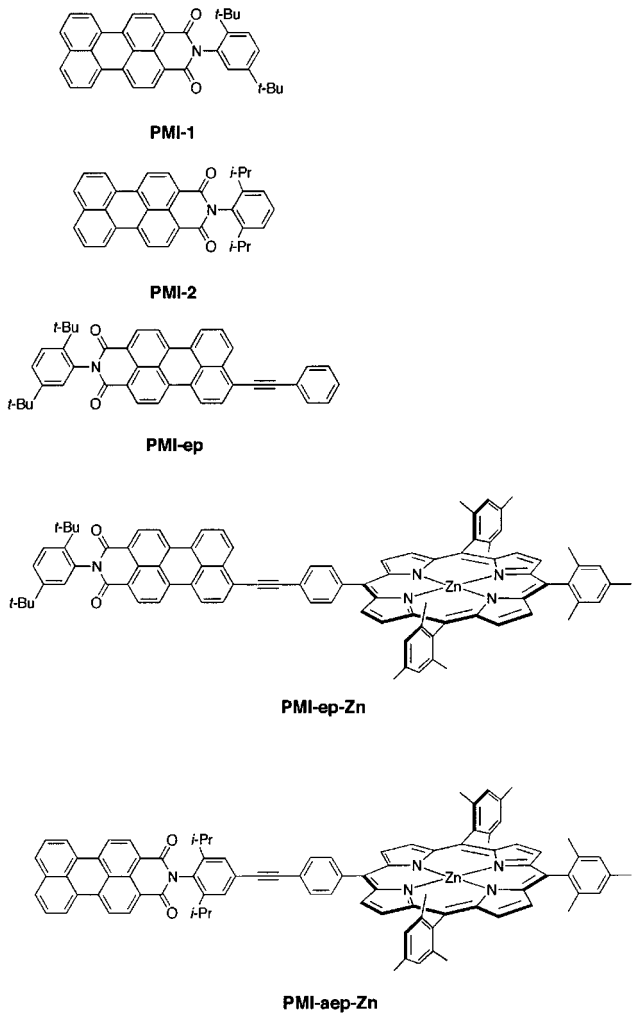

model systems have previously been prepared that incorporate perylene-monoimide dyes.[26] We exploited approaches for attaching a synthetic handle to a perylene-monoimide dye at either the *N*-imide position[18] or the C9 position.[23] The resulting perylene-monoimide (PMI) building blocks were employed to prepare the corresponding perylene-porphyrin dyads and relevant monomer reference compounds (Chart 3).

Each perylene-porphyrin dyad in toluene at room temperature exhibits fast and efficient energy transfer from perylene to porphyrin upon excitation of the perylene. The dyad **PMI-aep-Zn**, which employs a linker containing aryl (a), ethyne (e), and phenyl (p) groups, exhibits energy transfer from the photoexcited perylene-monoimide unit (PMI*) to the Zn porphyrin with $k_{trans} = (4.2\ ps)^{-1}$ (compared with the lifetime of 5.0 ns for **PMI-2**).[18] The dyad **PMI-ep-Zn** exhibits energy transfer from PMI* to the Zn porphyrin with $k_{trans} \geq (0.4\ ps)^{-1}$ (to be compared with the lifetime of 3.4 ns for **PMI-ep**), implying a yield of transfer $\Phi_{trans} > 99.8\%$.[17] The 10-fold difference in energy-transfer rates represents a major distinction between **PMI-aep-Zn** and **PMI-ep-Zn**. Additionally, the former exhibits a visible absorption spectrum that is the sum of the component parts while the latter does not. These distinctions have a structural/electronic basis in that the arylethynylphenyl linker at the *N*-imide position results in a weakly coupled system whereas the ethynylphenyl linker at the perylene C9 position results in a more strongly coupled system (albeit, the coupling is still relatively modest). Two perylene-monoimide dyes (**PMI-1**,[23] **PMI-2**[27]) have been prepared as benchmark monomers for the dyad **PMI-aep-Zn** (Chart 3). The dyes differ only in the nature of the solubilizing groups at the *N*-imide position, which causes little effect on photochemical properties.[28] To approximate the effects of linker groups in the more strongly coupled dyad, the perylene-monoimide dye **PMI-ep** is used as a benchmark.[14,17] Dyad **ZFbU**[6,12] (Chart 4) represents the output stage of each wire **1**−**4**.

The superior results obtained with the perylene-monoimide dye as a light absorber and energy-transfer donor (versus the BDPY dye) prompted us to prepare the analogous molecular photonic wire (**2**) with a perylene-monoimide dye as the input unit (Chart 1). We also prepared a shorter version of the wire containing only one Zn porphyrin between the perylene-monoimide dye and the Fb porphyrin (**3**). Both **2** and **3** are expected to be weakly coupled systems. For comparison, another short wire (**4**) was prepared that incorporates a more strongly coupled perylene input unit and an adjacent Zn porphyrin transmission element (the perylene-ep-porphyrin motif).

Herein, we describe the synthesis and photochemical properties of the new molecular wires **2**−**4**, as well as the original wire **1**. The synthesis and in-depth photochemical characterization of **1** have not been published previously, despite the fact that this wire served as the inspiration for a wide variety of studies of energy transfer in multiporphyrin arrays. The time-resolved investigations of **1**−**4** focus on the elucidation of the rates and efficiencies of end-to-end singlet−singlet excited-state energy transfer. Collectively, the studies provide detailed insight into the nature of excited-state electronic communication in these weakly coupled molecular photonic wires.

Results and Discussion

(A) Synthesis. The synthesis of the molecular wires was performed in a stepwise manner employing modular building blocks.[12] The key reaction for joining the building blocks is the Pd-mediated Sonogashira coupling of iodoaryl and ethynylaryl groups.[29] We have developed conditions for the Sonogashira coupling of an iodoarylporphyrin and an ethynylarylporphyrin in a 1:1 ratio in dilute solution (~2.5 mM) under mild conditions in the absence of any copper reagents.[30] Copper reagents are often employed in Sonogashira reactions but must be expressly avoided with Fb porphyrins, which readily undergo copper insertion. The ability to perform the coupling reaction in dilute solution is essential given the low solubility of the porphyrin building blocks.

(26) (a) Gosztola, D.; Niemczyk, M. P.; Wasielewski, M. R. *J. Am. Chem. Soc.* **1998**, *120*, 5118−5119. (b) Gensch, T.; Hofkens, J.; Heirmann, A.; Tsuda, K.; Verheijen, W.; Vosch, T.; Christ, T.; Basché, T.; Müllen, K.; De Schryver, F. C. *Angew. Chem., Int. Ed. Engl.* **1999**, *38*, 3752−3756. (c) Hayes, R. T.; Wasielewski, M. R.; Gosztola, D. *J. Am. Chem. Soc.* **2000**, *122*, 5563−5567. (d) Just, E. M.; Wasielewski, M. R. *Superlatt. Microstr.* **2000**, 28, 317−328.

(27) Quante, H.; Müllen, K. *Angew. Chem.* **1995**, *107*, 1487−1489.

(28) Langhals, H.; Demmig, S.; Huber, H. *Spectrochim. Acta* **1998**, *44A*, 1189−1193.

(29) Sonogashira, K.; Tohda, Y.; Hagihara, N. *Tetrahedron Lett.* **1975**, 4467−4470.

(30) Wagner, R. W.; Ciringh, Y.; Clausen, P. C.; Lindsey, J. S. *Chem. Mater.* **1999**, *11*, 2974−2983.

Chart 4

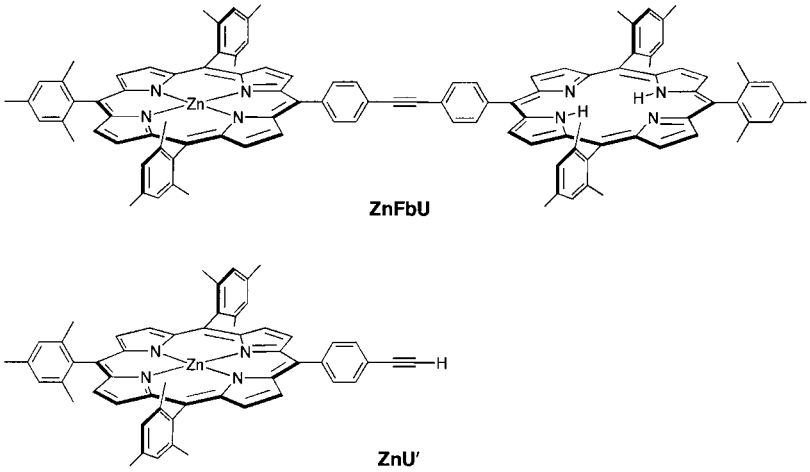

In principle, the synthesis can proceed in either direction along the wire, from input to output unit or from output to input unit. The choice of direction dictates the nature of the synthetic handles on the various building blocks. We elected to perform the synthesis from output to input unit for two reasons. First, we sought to attach different input units, which could be done in the last step of a synthesis performed in the direction from output to input. Second, preliminary studies indicated a need to minimize handling of the BDPY input unit. Accordingly, the requisite building blocks include an ethynyl Fb porphyrin, a Zn porphyrin bearing a TMS-ethyne group and an iodo group, and an iodo-substituted BDPY dye or a bromo-substituted perylene-monoimide dye.

The coupling reactions were carried out under mild conditions using $Pd_2(dba)_3$ and P(*o*-tol)$_3$ in toluene/triethylamine (5:1) at 35 °C under an inert atmosphere using Schlenk-line techniques. The progress of the reaction was monitored by analytical size-exclusion chromatography (SEC) and laser desorption mass spectrometry (LD-MS). Each step in the synthesis of molecular wires **1** and **2**, except for the last step of each, was performed in at least two separate batches. The batches were purified separately, and then the products from each were combined prior to performing the next reaction. This approach enabled a check on the robustness of the yield of each reaction as well as a fallback mechanism in the event of failure of any reaction in the linear synthetic plan.

The first steps in the synthesis leading to **1** and **2** are shown in Scheme 1. The Fb ethynylphenylporphyrin[31] **FbU′** and the Zn porphyrin bearing both iodophenyl and trimethylsilylethynylaryl groups (**5**)[12] were reacted (0.40 mmol of each) under the Pd-mediated coupling conditions. Analytical SEC showed a major peak corresponding to the desired dyad and a shoulder due to the faster eluting, higher molecular weight material. Purification of the dyad from the crude reaction mixture involved a sequence of four chromatographic procedures: (1) silica gel chromatography to afford a mixture of porphyrin components free from P(*o*-tol)$_3$ and Pd species; (2) preparative SEC in toluene or THF, which affords separation of the starting material, desired dyad, and most of the higher molecular weight material; (3) a second preparative SEC to remove the closely moving higher molecular weight material from the desired dyad; and (4) final cleanup by silica gel chromatography to give the desired dyad. The composition of the fractions was assessed by analytical SEC at all stages of the purification process. In this manner, the pure dyad **6** was isolated in 52% yield. Two additional runs afforded dyad **6** in yields of 56% and 46%.

The trimethylsilyl group of **6** was cleaved using Bu_4NF (TBAF) on silica in THF, affording dyad **6′** bearing a free ethyne group in 96% yield. Purification entailed a water wash and chromatography over a short silica column. A second run afforded the same dyad in 92% yield.

The synthesis was continued using the two-step sequence of Pd-coupling and deprotection of the trimethylsilylethyne group. In this manner, the reaction of ethynyl-dyad **6′** and porphyrin **5** afforded triad **7** in 44% yield (average), which upon deprotection afforded ethynyl-triad **7′** in 94% yield (average). The similar reaction of **7′** and **5** gave the desired tetrad **8** in 39% yield (average). Deprotection of the trimethylsilyl group in tetrad **8** required use of toluene/THF (4:1) as solvent, affording ethynyl-tetrad **8′** in 90% yield (average).

The coupling reaction of ethynyl-tetrad **8′** and the iodophenylboron-dipyrrin dye[13] **9** was carried out to obtain the desired molecular wire **1** (Scheme 2). The desired pentad (**1**) and the unreacted tetrad (**8′**) co-chromatographed upon preparative SEC. The analytical SEC trace showed that the two compounds differ in their retention time by approximately 0.1 min. The crude mixture containing **1** and unreacted **8′** (but very little higher molecular weight material of the type typically formed in the Pd-coupling reactions of two porphyrins) was separated by column chromatography on silica gel with toluene/hexanes (4:1). The desired molecular wire **1** was obtained in 71% yield. The overall yield (based on available building blocks) for the synthesis of **1** is 4.9%. The yields of the Pd-coupling reactions of **5** + the nascent wire (**6′**, **7′**, **8′**) declined slightly during the course of the synthesis (51%, 44%, 39%), while the TMS deprotection steps remained above 90% in all cases. A summary of the amount of the starting material, product, and yields at each step in this synthetic sequence is provided in a table in the Supporting Information.

The perylene-based molecular wire was prepared by reaction of the ethynyl-tetrad **8′** and the bromo-substi-

(31) Wagner, R. W.; Johnson, T. E.; Li, F.; Lindsey, J. S. *J. Org. Chem.* **1995**, *60*, 5266−5273.

Scheme 1

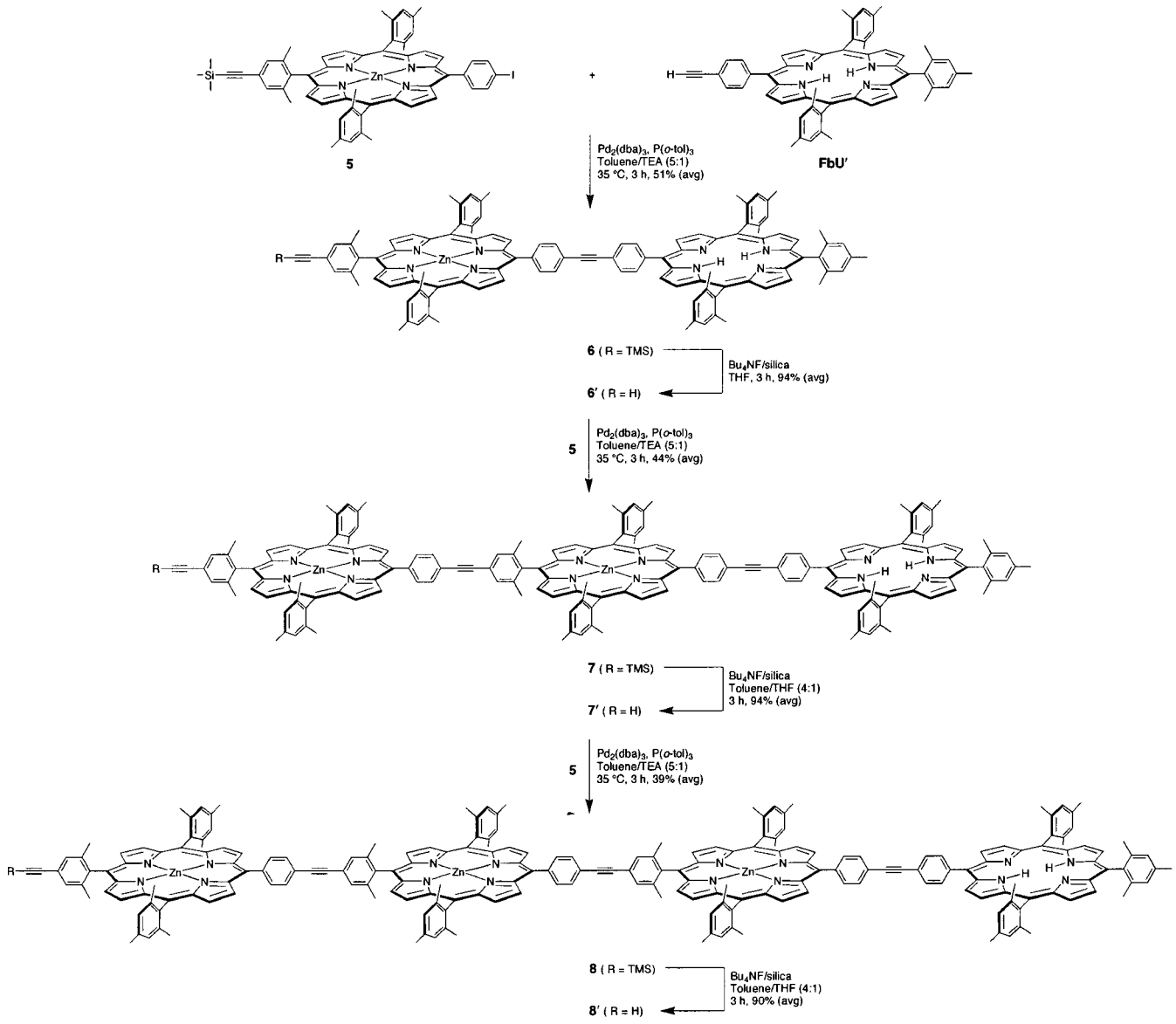

Scheme 2

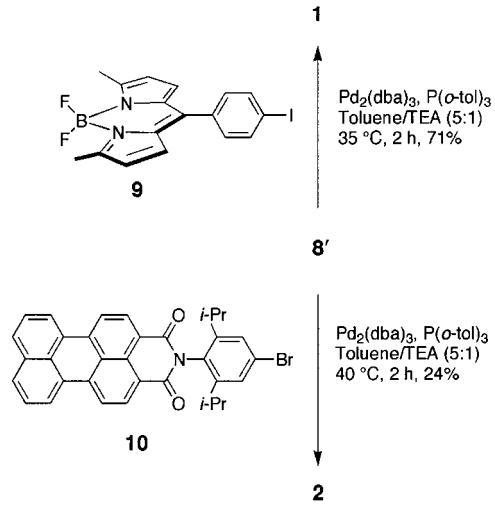

Scheme 3

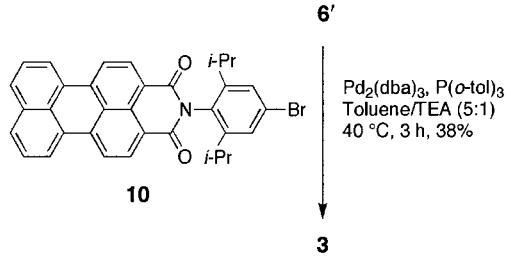

tuted perylene-monoimide[18] **10** (Scheme 2). The bromo + ethyne coupling reaction[32] proceeds under essentially the same conditions as for the iodo + ethyne reaction, though typically at slightly higher temperature. Thus, the reaction of **10** and **8′** in a 1:1 ratio at 40 °C afforded the molecular wire **2** in 24% yield following chromatographic purification. ^{1}H NMR spectroscopy of **2** could not be performed due to the low solubility of the sample in solvents such as toluene, THF, and dichloromethane.

The homologous perylene-based wire with only one Zn porphyrin was synthesized as shown in Scheme 3. The reaction of ethynyl-dyad **6′** and bromoperylene-monoim-

(32) Loewe, R. S.; Lammi, R. K.; Diers, J. R.; Kirmaier, C.; Bocian, D. F.; Holten, D.; Lindsey, J. S. *J. Mater. Chem.* **2002**, *12*, 1530−1552.

Scheme 4

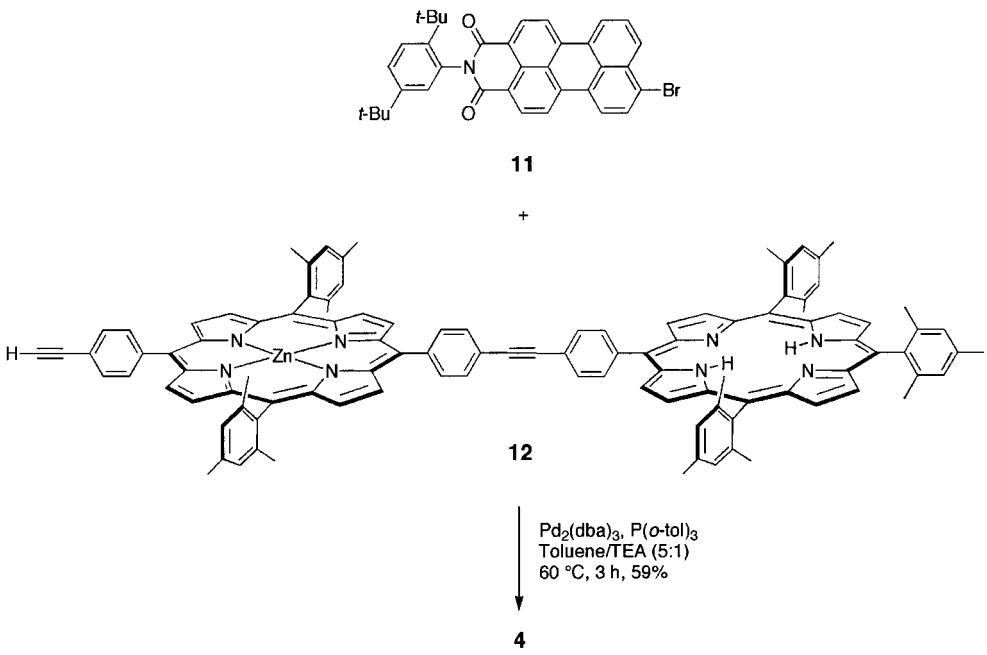

ide **10** at 40 °C afforded the perylene-based short wire **3** in 38% yield.

The more strongly coupled analogue of the perylene-based short wire was prepared as shown in Scheme 4. The reaction of ethynyl-dyad **12** and bromoperylene-monoimide **11**[23] under the Pd-coupling conditions at 60 °C afforded the desired molecular wire **4** in 59% yield.

In general, the products of each synthetic reaction were characterized by analytical SEC, LD-MS, UV−vis absorption spectroscopy, fluorescence spectroscopy, and ^{1}H NMR spectroscopy. The addition of each Zn porphyrin to the nascent wire was readily observed by the change in the visible absorption spectrum, given that the absorption in the visible region is the sum of the spectra of the Fb porphyrin and the Zn porphyrins. The addition of the input units also was readily observed by absorption spectroscopy, though in the case of the ethynylphenyl-linked perylene wire (**4**) the absorption spectrum of the perylene-ep-Zn porphyrin is slightly red shifted from the sum of the spectra of the component parts.

Solubility. Solubility of the arrays in a variety of solvents is essential for synthesis, purification, and chemical characterization. The dyads **6** and **6′** were soluble in toluene at room temperature. The triads (**7**, **7′**) and tetrads (**8**, **8′**) were soluble at 2.5 mM in toluene/TEA (5:1) at 35 °C, as required for carrying out the Pd-coupling reactions. In general, the crude reaction mixture after a Pd-coupling or a TMS-deprotection reaction was dissolved in a minimum amount of toluene or THF by warming in a hot water bath at 45 °C for a few minutes prior to chromatographic purification. In most cases, a 5-mg sample of an array could be dissolved in 0.5 mL of $CDCl_3$ for routine NMR measurements.

(B) Photophysical Properties and Energy-Transfer Dynamics. Ground-State Absorption Spectra. Electronic absorption spectra for wires **1**−**4**, dyad **ZnFbU**, and reference compounds **FbU′**, **ZnU′**, **PMI-2**, and **BDPY-TMS** (Charts 1−4) are given in Figure 1 (solid spectra).

The spectra of the **FbU′** and **ZnU′** porphyrin monomers (Figure 1F,G) contain the intense near-UV Soret band (420−425 nm) and a series of weaker visible Q bands (500−660 nm). The Q(2,0), Q(1,0), and Q(0,0) bands of the Zn porphyrin at 510, 550, and 590 nm, respectively, correspond to transitions from the ground state to the lowest excited singlet state Zn*. Due to the reduced symmetry, these bands split into the Q_Y(2,0), Q_Y(1,0), Q_Y(0,0), Q_X(1,0), and Q_X(0,0) bands of the Fb porphyrin at 485, 515, 550, 590, and 650 nm, respectively, the latter two features reflecting excitation to the lowest excited singlet state Fb*. (The weak Q_X(2,0) band of the Fb porphyrin is buried under the Q_Y features.)

The spectrum of the perylene-monoimide reference compound **PMI-2** (Figure 1H) has a series of four overlapping features at 506, 479, 455, and 425 nm that correspond to the (0,0), (1,0), (2,0), and (3,0) transitions from the ground state to the lowest excited singlet state PMI*. This spectrum is virtually identical to that of the related perylene-monoimide dye **PMI-1** studied previously[17] that differs in the aryl group on the imide nitrogen (Chart 3). The spectrum of the boron-dipyrrin dye, **BDPY-TMS** (Figure 1I), has a strong (0,0) absorption band at 516 nm and a shoulder of about one-third the amplitude at 485 nm.[13]

The Q-band spectral region for dyad **ZnFbU** (Figure 1E) is the sum of spectra of the reference monomers (Figure 1F,G).[6,33,34] This observation, together with the finding of similar redox potentials in the dyad and monomers,[10] reflects the relatively weak electronic interactions between diarylethyne-linked porphyrins in the ground state and in the photophysically key lowest excited singlet states. The spectrum of **ZnFbU** in the Soret region (involving transitions to higher excited states) has contributions from both porphyrins, including splitting due to coupling of their strong Soret transition dipoles.

(33) Hsiao, J.-S.; Krueger, B. P.; Wagner, R. W.; Johnson, T. E.; Delaney, J. K.; Mauzerall, D. C.; Fleming, G. R.; Lindsey, J. S.; Bocian, D. F.; Donohoe, R. J. *J. Am. Chem. Soc.* **1996**, *118*, 11181−11193.

(34) Strachan, J. P.; Gentemann, S.; Seth, J.; Kalsbeck, W. A.; Lindsey, J. S.; Holten, D.; Bocian, D. F. *J. Am. Chem. Soc.* **1997**, *119*, 11191−11201.

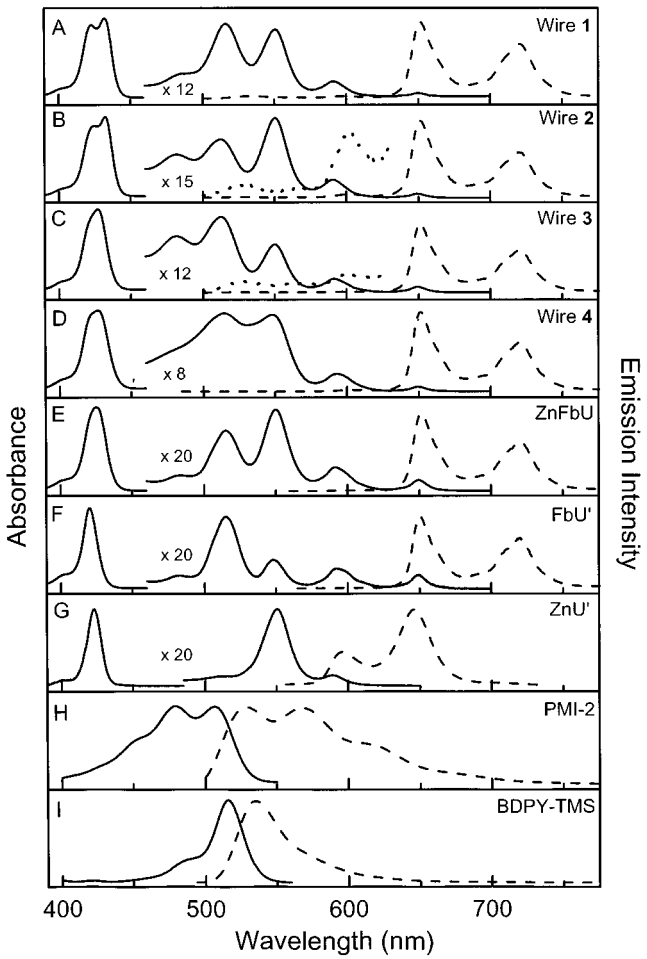

Figure 1. Room-temperature absorption (solid) and emission (dashed, dotted) spectra of the wires and reference compounds in toluene. The porphyrin Q-regions of the absorption spectra in A−F have been multiplied by the factors indicated. The dotted emission traces in B and C have been multiplied by a factor of 20 from the dashed spectra.

The absorption spectrum of wire **3** is the sum of the spectra of the **ZnFbU** dyad and PMI monomer **PMI-2** (Figure 1C). This result reflects the relatively weak electronic interactions between the arylethynylphenyl-linked PMI input unit and the Zn porphyrin transmission element. The contribution of the PMI unit between 430 and 530 nm causes the features near 485 and 515 nm in **3** to be more intense than the band at 550 nm (due mainly to the Zn porphyrin), whereas the relative absorbances at 485 (or 515) and 550 nm are reversed in **ZnFbU** (Figure 1C,E). These findings (and the relative extinction coefficients) indicate that the perylene unit of wire **3** absorbs ~85% of the light in the vicinity of 485 nm, allowing for reasonably selective excitation of the input unit.

This selectivity is retained in wire **2**, which is a longer analogue of **3**, containing three rather than one Zn porphyrin transmission elements (Chart 1). The spectrum of **2** (Figure 1B) is generally well described by adding the absorption of two more Zn-porphyrin units (Figure 1G) to the spectrum of **3** (Figure 1C). This aspect is most apparent from the increased contribution of the Zn porphyrin Q(1,0) absorption at 550 nm relative to the other bands. The long-wavelength half of the Soret absorption of **2** also grows in intensity relative to **3** due to the increased contribution of the Zn porphyrins and the exciton coupling between them.

The absorption properties of wire **1** can be understood based on those of wire **2** and the change in the input unit from a perylene to a boron-dipyrrin (BDPY) pigment. Comparison of the spectra of **1** and **2** (Figure 1A,B) shows that they differ in the absorption of the input units between 450 and 550 nm (Figure 1H,I). The prominent BDPY band at ~515 nm (~40% stronger than the perylene bands at ~505 and ~485 nm) causes the combined absorption at 515 nm in **1** to be greater than the feature at 550 nm (which is due primarily to the three Zn porphyrins), whereas the opposite is true in **2**. On the basis of the relative contributions of the components, the BDPY input unit in **1** absorbs over half of the light at 515 nm and at 485 nm, allowing for preferential excitation of the input unit. Analogous to the situation for PMI-based wires **2** and **3**, the blue-green absorption properties of wire **1** reflect the relatively weak interactions between the BDPY input unit and the first Zn porphyrin transmission element.

The modest electronic interactions involving the input and transmission element(s) in wires **1**−**3** can be contrasted to the situation in wire **4** (Chart 1). Wire **4** differs from **3** in the use of an ethynylphenyl (ep) versus arylethynylphenyl (aep) linker and the attachment of the linker at the perylene C9 versus the *N*-imide position. The consequences on the absorption properties can be seen by comparing the spectra of these two wires with each other (Figure 1C,D) and with their building blocks (e.g., Figure 1E,H). One of the most notable characteristics is that the absorption features of the PMI unit in **4** are broadened and red shifted by ~35 nm from their positions in the PMI monomer **PMI-2**. The result is that the perylene absorption overrides the porphyrin (primarily Fb) absorption at 515 nm and substantially overlaps the porphyrin (primarily Zn) contribution 550 nm. We have noted similar effects in our previous studies of dyad **PMI-ep-Zn** (Chart 3), which employs the same perylene and connectivity to the Zn porphyrin in wire **3**.[17,35]

Fluorescence Spectra and Quantum Yields. The emission spectra for wires **1**−**4** and their component subunits in toluene at room temperature are shown in Figure 1 (dashed and dotted lines).

The fluorescence emission for **BDPY-TMS** consists of a main feature at 535 nm and a shoulder to longer wavelengths, in agreement with previous measurements (Figure 1I).[7,13] This pigment has a fluorescence quantum yield of 0.058.[7] The fluorescence bands of the **PMI-2** monomer are roughly in mirror image to the corresponding absorption bands, with (0,0) and (0,1) emission features at 528 and 567 nm having comparable intensity and the progressively weaker (0,2) and (0,3) features at 620 and 780 nm (Figure 1H). These emission properties are essentially the same as those found previously for the closely related perylene-monoimide dye **PMI-1** (Chart 3), which has a fluorescence quantum yield of 0.99.[17] The attachment of the ethynylphenyl group at the C9 position red shifts the emission features of **PMI-ep** (not shown)

(35) Our previous studies on **PMI-ep-Zn** and related dyads revealed that the absorption (and emission) properties of the porphyrin are affected by coupling via the ep linker to the perylene at its C9 position (but not as substantially as those of the perylene).[17] The same is likely to be true in wire **4**, although modest changes in the optical properties of the Zn porphyrin are difficult to assess in this case due to overlap with features from the Fb porphyrin output unit.

by ~30 nm from those in **PMI-1** (and thus from **PMI-2** in Figure 1H).[17]

The **ZnU′** emission has rough mirror symmetry to the absorption spectrum and is dominated by the Q(0,0) and Q(0,1) bands at 598 and 647 nm (Figure 1G). Likewise, the fluorescence of **FbU′** primarily occurs in two bands, namely the $Q_Y(0,0)$ and $Q_Y(0,1)$ features at 650 and 720 nm (Figure 1F). The emission of the corresponding Fb porphyrin output unit in turn dominates the spectra of **ZnFbU** and wires **1**−**4** (Figures 1A−E), irrespective of which component in each of these arrays is excited, as is described in the following.

Dyad **ZnFbU** in toluene shows essentially no emission from the Zn porphyrin even when this component is primarily excited (e.g., at 550 nm).[6,33,36] Furthermore, measurements on matched samples of **ZnFbU** and **FbU′** at 550 or 435 nm show that the emission yield from the Fb porphyrin unit is the same within error as the value of $\Phi_f = 0.12 \pm 0.01$ for the **FbU′** monomer, in agreement with our previous studies (see the Supporting Information).[37] The results for **ZnFbU** in toluene, like similar static emission and time-resolved results described previously, are indicative of (1) essentially quantitative energy transfer from the Zn porphyrin to the Fb porphyrin via the diphenylethyne linker and (2) a lack of subsequent quenching of the excited Fb porphyrin by the appended Zn porphyrin by processes such as charge transfer. These findings provide a reference point for assessing the emission data for wires **1**−**4**, particularly the extent of energy transfer from the Zn-porphyrin transmission element(s) to the Fb porphyrin output unit.

The emission from "short" wires **3** and **4**, both of which contain only one Zn porphyrin transmission element, also occurs almost exclusively from the Fb porphyrin even when the perylene input unit is preferentially pumped in the region of its (1,0) absorption band (460−490 nm). These results are evident from the (1) fluorescence spectra for these wires (Figure 1C,D, dashed) when compared with those for the monomers (Figure 1F−H), and (2) the emission intensities for the wires compared to those of the reference compounds. Only trace emission is observed from the Zn porphyrin in either **3** or **4**, as can be seen from the minor intensity in ~600 nm in the expanded view shown for **3** in Figure 1C (dotted). Indeed, a fraction of this intensity actually corresponds to the perylene emission that extends to shorter wavelengths (see Figure 1H). The minor perylene emission in **3** and **4** is reduced about 1000-fold from that observed in the **PMI-1**, **PMI-2**, and **PMI-ep** monomers, which are bright emitters with near-unity fluorescence yields, as described above. Furthermore, the intensity of the Fb porphyrin emission in **3** and **4** in toluene is undiminished compared to that of **FbU** (or **ZnFbU**) when either the perylene or Fb porphyrin is excited (after correcting for absorbance at the excitation wavelength). These combined findings are diagnostic of highly efficient energy transfer from the excited PMI input unit to the Zn porphyrin transmission element and then on to the Fb porphyrin output unit in wires **3** and **4**. That this energy-transfer process is virtually quantitative is derived from the time-resolved absorption measurements described below.

Emission also occurs primarily, but not exclusively, from the Fb porphyrin output unit in the longer wires **1** and **2**, each of which has three rather than one Zn porphyrin in the transmission chain (Chart 1). Wire **2** has the same PMI input unit and connectivity present in **3**, while **1** employs a BDPY input unit. The amount of energy that is ultimately emitted by the Fb porphyrin following excitation of the input unit is reduced modestly for long wires **1** and **2** compared to short wires **3** and **4** (and **ZnFbU** and **FbU′**). This conclusion is derived from two main methods, namely (1) assays based on the static emission spectra and emission intensities, and (2) excited-state lifetimes derived from the time-resolved absorption data (vide infra). The various assays based on the static emission properties are interrelated and include the following: (1) A comparison of emission intensities for the various arrays using a number of excitation wavelengths and detection windows that probe the emission from the perylene, the Zn porphyrins, or the Fb porphyrin in order to assess the overall energy-transfer efficiency and the efficiency at each stage. (2) Simulation of the overall emission spectrum of the wire using the absorption and emission properties of the constituent monomers in order to deduce an overall transfer efficiency. Detailed descriptions of these static emission analyses are given in the Supporting Information, along with those for the time-resolved measurements described in subsequent sections. We find these methods for static emission to be preferable to comparisons of the absorption and fluorescence excitation spectra[38] for estimating energy-transfer efficiencies. The salient points concerning energy-transfer efficiencies derived from the static emission assays are described below: We begin with a discussion of the end-to-end energy transfer and then proceed to the discussion of transfer in the individual stages of the wires.

(1) An overall efficiency of 83% ± 7% in wire **2** is obtained by measuring the Fb porphyrin emission intensity upon excitation of the perylene input unit (460 or 470 nm) relative to the quantitative level found from **FbU′** (and **ZnFbU** and the short wires **3** and **4**). A second estimate for the overall efficiency of 80−89% in wire **2** is obtained from simulations of the emission spectrum from the known absorption and emission profiles and emission yields of all the components using the program PhotochemCad.[39] A set of simulations on wire **1** give an overall efficiency of ~73% (76% was reported earlier;[1] see the Supporting Information).

(2) The reduced Fb porphyrin emission observed following PMI-input-unit excitation in **2** does not derive from diminished energy transfer to the adjacent Zn porphyrin (relative to the essentially quantitative level found in **3** and **4**). This is evidenced by the fact that trace fluorescence is seen from PMI in **2**. For example, comparable amounts of PMI (0,0) fluorescence are observed in the vicinity of 530 nm for wires **2** and **3** in the expanded views in Figure 1B,C (dotted). As noted above

(36) Dyad **ZnFbU** shows only trace intensity above the baseline in the vicinity of the Zn porphyrin Q(0,0) band at ~600 nm, where the Fb porphyrin does not emit. Similarly, there is minimal Zn porphyrin emission in its stronger Q(0,1) band, which if present would substantially overlap the $Q_X(0,0)$ emission of the Fb porphyrin at 650 nm and alter the intensity relative to the $Q_X(0,1)$ band at 720 nm; however, the intensity ratio in the **ZnFbU** dyad is the same as in the **FbU′** monomer (Figure 1E,F).

(37) Yang, S. I.; Seth, J.; Strachan, J.-P.; Gentemann, S.; Kim, D.; Holten, D.; Lindsey, J. S.; Bocian, D. F. *J. Porphyrins Phthalocyanines* **1999**, *3*, 117−147.

(38) Stryer, L.; Haugland, R. P. *Proc. Natl. Acad. Sci. U.S.A.* **1967**, *58*, 719−726.

(39) Du, H.; Fuh, R.-C. A.; Li, J.; Corkan, L. A.; Lindsey, J. S. *Photochem. Photobiol.* **1998**, *68*, 141−142.

for **3** (and **4** and **PMI-ep-Zn**[17]), the trace perylene emission in **2** is reduced ~1000-fold from that of the **PMI-2** reference compound and is only observed because of the inherent near-unity fluorescence yield of the pigment in the absence of energy transfer.

(3) The Fb porphyrin emission observed following BDPY-input-unit excitation in **1** derives in part from diminished energy transfer to the adjacent Zn porphyrin compared to the PMI-based wires. Indeed, the amount of residual emission observed from the BDPY chromophore is larger than that from the PMI input unit in the other wires despite a 17-fold lower intrinsic fluorescence yield (0.058 vs 0.99). Quantitation of this point is more easily accomplished in the **BDPY-Zn** dyad, where we have previously measured a BDPY emission yield of 0.002 compared to 0.058 for **BDPY-TMS**, corresponding to a BDPY → Zn energy-transfer efficiency of 97%.[7]

(4) The reduced Fb porphyrin emission observed following excitation of the input units in **1** and **2** does not derive to any significant extent from quenching of the output unit once the latter receives energy from the Zn-porphyrin transmission chain. This conclusion derives from the finding that the emission of the Fb porphyrin in **1** and **2** obtained upon direct excitation of this unit (640 and 650 nm) is undiminished from that in **3**, **4**, **ZnFbU**, and **FbU′**.

(5) The above observations indicate that modestly reduced Fb porphyrin emission found after input-unit excitation in long wires **1** and **2** compared to short wires **3** and **4** must derive largely (in **1**) or essentially exclusively (in **2**) from nonquantitative energy transfer from the three-unit Zn-porphyrin transmission chain to the Fb porphyrin. This deduction is confirmed by direct observation. In particular, although the Zn-porphyrin emission is reduced dramatically (≥15-fold) in all the wires compared to reference monomers such as **ZnU′**, the residual amount is about 7-fold greater for the two long wires **1** and **2** compared to the short wires **3** and **4** (and **ZnFbU**). This general result can be seen from the larger Zn-porphyrin (0,0) emission near 600 nm (above the trace perylene emission) in **2** versus **3** in the expanded view in Figure 1B,C (dotted). When quantitated, the observed residual Zn porphyrin emission suggests that the net efficiency of energy transfer from the Zn porphyrin transmission elements to the Fb porphyrin in wire **2** is 80 ± 10% of that in **3**.

The results of the static emission assays will be combined below with those from the time-resolved measurements that are described next in order to arrive at consensus estimates for end-to-end energy-transfer efficiencies in wires **1** and **2**.

Transient Absorption Spectra and Kinetics. Time-resolved absorption studies were conducted on wires **1**−**4** (Chart 1) in toluene, using 130-fs excitation flashes at 480−490 nm that primarily pump the input unit (BDPY or PMI). For comparison, selected transient spectra for the perylene monomer **PMI-2** and the perylene-porphyrin dyad **PMI-aep-Zn** (Chart 3) in toluene are also given (the full photophysical characterization of these two molecules will be presented elsewhere[18]).

The absorption difference spectrum of the lowest excited singlet state (PMI*) of perylene reference compound **PMI-2** is shown in Figure 2A (solid). The spectrum shows a broad trough between 500 and 550 nm that contains bleaching of the perylene (1,0) and (0,0) ground-state absorption bands as well as PMI* (0,0) stimulated

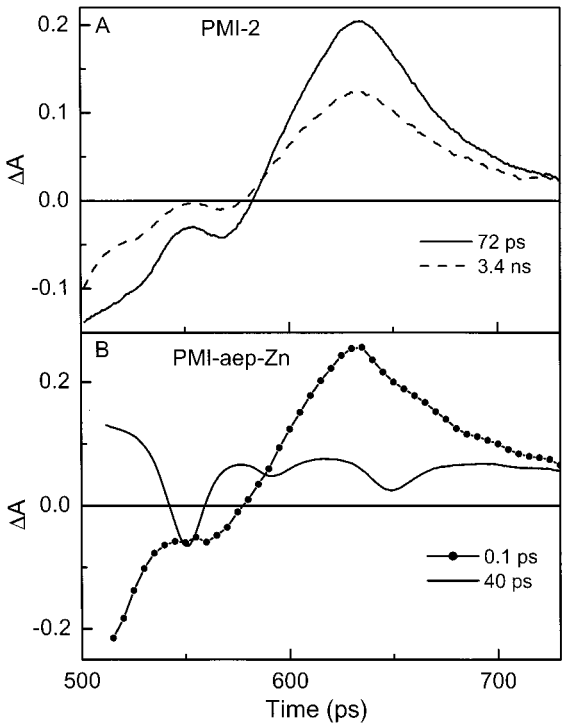

Figure 2. Absorption difference spectra at selected probe−pump time delays for perylene monomer **PMI-2** (A) and perylene−porphyrin dyad **PMI-aep-Zn** (B) in toluene at room temperature obtained using 130-fs excitation flashes at 485 nm (which primarily pump the input unit in the array).

emission, while the dip at 570 nm is (0,1) stimulated emission (fluorescence stimulated by the white light probe pulse). These features coincide with related bands in the static absorption and spontaneous fluorescence spectra (Figure 1H). The PMI* spectrum also exhibits a broad, strong absorption band (involving transitions to higher excited singlet states) centered at 635 nm. All of the PMI* features have uniformly and partially decayed by the 3.4 ns limit of the spectrometer (Figure 2A, dashed). Assuming that the spectrum would continue to decay to the $\Delta A = 0$ baseline, a PMI* lifetime of ~5 ns is estimated. [This is a good assumption given that perylene-imides decay primarily by fluorescence (to the ground state) with minimal formation of the excited triplet state.[15−17]] This value compares well with that of 5.0 ns obtained from fluorescence lifetime studies of this compound.[18]

Excitation of the perylene unit in dyad **PMI-aep-Zn** affords the PMI* absorption difference spectrum shown at 0.1 ps after excitation in Figure 2B. This spectrum is in excellent agreement with that for **PMI-2** (Figure 2A) even though it is constructed from the raw data due to fast PMI* decay in the dyad and convolution with temporal dispersion of wavelengths in the probe pulse.[40] The excited perylene in **PMI-aep-Zn** decays with a lifetime of 4.2 ± 0.3 ps, which is over 1000-fold shorter than the PMI* lifetime in **PMI-2**. This finding reflects the highly efficient energy transfer from the photoexcited

(40) The PMI* spectra for the arrays were obtained from the initial amplitudes of the absorbance changes at each wavelength because the early time spectra are slightly distorted due to the convolution of the fast PMI* decay and the temporal dispersion of the wavelengths in the white-light probe pulse. In the wires, the spectra were obtained using the preexponential factor for the associated component from the multiexponential fits of the kinetic data.

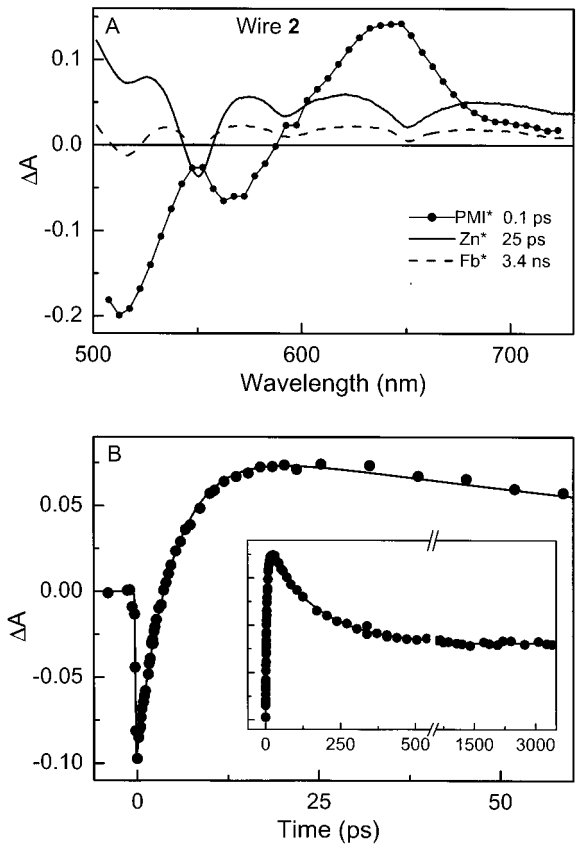

Figure 3. Absorption difference spectra (A) and a kinetic profile and fit (B) for wire **2** obtained under the conditions described in Figure 2. The fit to the kinetic data at 515 in (B), with the full time window of the measurement in the inset, is the convolution of the instrument response with a dual exponential plus a constant, giving time constants of 5 ps (PMI* decay) and 150 ps (Zn* decay). The average time constants derived from the kinetic data across the spectrum are given in Table 1.

perylene unit to the ground-state Zn porphyrin to form Zn* in the dyad (denoted PMI* → Zn). This process is accompanied by decay of the PMI bleaching and PMI* stimulated emission and excited-state absorption features and the formation of the Zn* characteristics (Figure 2B, solid). The Zn* absorption difference spectrum contains several features embedded on the broad excited-state absorption, notably bleaching of the Zn porphyrin ground state (0,1) band at 550 nm, (0,0) bleaching and Zn* stimulated emission at 595 nm, and (0,1) stimulated emission at 645 nm. This spectrum then evolves modestly over the next several nanoseconds as Zn* decays (primarily by intersystem crossing to the triplet state) basically as in the isolated **ZnU′** monomer.

Representative time-resolved spectral data for long wire **2** are shown in Figure 3. The PMI* spectrum shown at 0.1 ps after direct excitation of this component in wire **2** is virtually identical to those found in **PMI-2** and **PMI-aep-Zn** (Figure 2). The PMI* decay in the wire is accompanied by formation of Zn* (Figure 3A, solid) with spectral characteristics identical to those of Zn* in **PMI-aep-Zn** (Figure 2B, solid). Unlike the situation in the dyad, Zn* decays over the next several hundred picoseconds in **2** to give spectral features characteristic of Fb* (Figure 3A, dashed). The Fb* spectrum consists of a broad excited-state absorption and a group of features consistent with the related bands in the static optical spectra

Table 1. Summary of Excited-State Lifetimes and Energy-Transfer Efficiencies[a]

compd	excited-state lifetime (ps) PMI* or BDPY*	Zn*	Φ_{trans}[b] (%)
wires			
1	25 ± 5, 1.7 ± 0.4[c]	160 ± 30	81 ± 9
2	5.3 ± 0.8	170 ± 30	86 ± 7
3	5.2 ± 0.8	28 ± 3	99
4	≤0.4	26 ± 3	99
dyads			
ZnFbU		24 ± 2[d]	99
PMI-ep-Zn	≤0.4[e]		>99
PMI-aep-Zn	4.2 ± 0.3[f]		>99
BDPY−Zn	16 ± 1, 1.8 ± 0.4[c,g]		94
monomers			
ZnU′		2400 ± 200[h]	
PMI-2	~4500		
PMI-1[i]	4800 ± 100[e]		
PMI-ep	3400 ± 100[e]		
BDPY-TMS	520 ± 50; 15 ± 4[g]		

[a] All measurements in toluene and room temperature. [b] The efficiency is the average of values obtained from several assays (see text). [c] BDPY has two excited-state conformers that have different lifetimes in the isolated pigment and different energy-transfer rates with an attached porphyrin. The slow component comprises 80% of the decay in **1** and 70% in **BDPY−Zn**. [d] References 6 and 33. [e] Reference 17. [f] Reference 18. [g] Reference 7. [h] References 33 and 37. [i] Formerly called **PMI-m** in ref 17.

(Figure 1F), namely bleaching of the ground-state Q bands at approximately 515, 550, 595, and 650 nm and stimulated emission near 650 and 720 nm. The time profile at 515 nm in Figure 3B shows the decay of the PMI bleaching and formation of the Zn* excited-state absorption, followed by partial decay of this transient absorption as Zn* gives way to Fb*. The data at this wavelength and others across the spectrum yield a PMI* lifetime of 5.3 ± 0.8 ps and a Zn* lifetime of 170 ± 30 ps (Table 1). This Zn* lifetime is considerably shorter than the value of 2.4 ns observed in the isolated Zn porphyrin **ZnU′**, reflecting efficient energy transfer to the Fb porphyrin.

The transient absorption spectral and kinetic data for wire **3**, the short analogue of **2**, are shown in Figure 4. The spectrum of the excited PMI input unit observed immediately after excitation (solid circles) and the spectrum of the excited Fb porphyrin output unit observed at ~100 ps and longer times (dashed) are both comparable in detail to those found for **2**. The major difference in the spectral evolution is that there is no intermediate time at which a "pure" Zn* spectrum is observed. For example, the spectrum for **3** at 20 ps (Figure 4A, solid) contains all the Zn* characteristics seen in **2** and **PMI-aep-Zn** (see Figures 2B and 3A, solid) but clearly has extra bleaching at 515 nm because some Fb* has already begun to form from Zn*. This situation reflects the fact that the residence time of the energy on the single Zn porphyrin transmission element in **3** is much shorter than that for the chain of the three Zn porphyrins in **2** (Chart 1). This difference is also seen in the fact that the Zn* lifetime of 28 ± 3 ps found for **3** is five times shorter than the value of 170 ps for **2** (compare decay profiles at 515 nm in the inset to Figure 3 and the main panel of Figure 4). The Zn* decay time for **3** is in excellent agreement with the value of 24 ± 2 ps observed previously in **ZnFbU**, which has the same connectivity between the Zn and Fb porphyrins (Charts 1 and 4).[6,33,34] This agreement is even better when it is recognized that the time constant of the second kinetic component

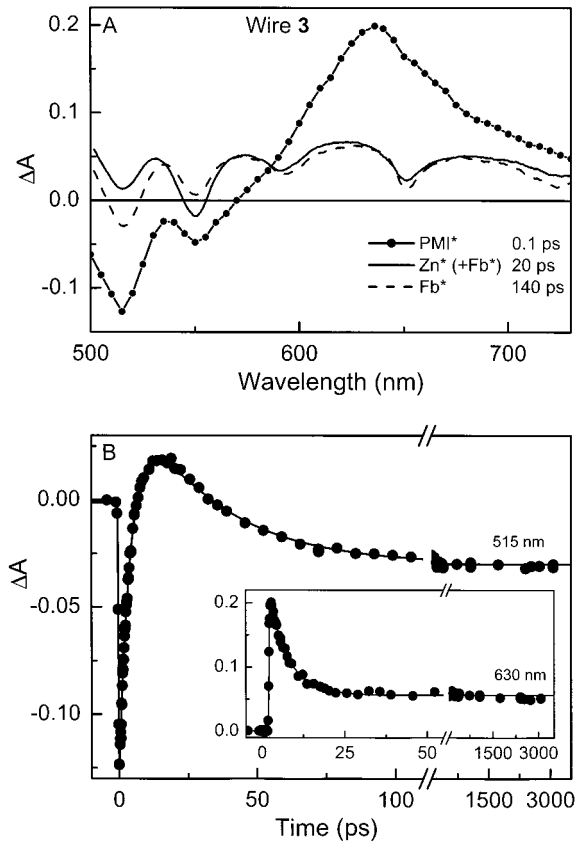

Figure 4. Time-resolved absorption data for wire **3** analogous to those described for wire **2** in Figure 3. The dual-exponential fit to the kinetic trace at 515 nm in the main panel in (B) gives time constants of 4.5 and 30 ps; the profile at 630 nm in the inset give 5.7 and 25 ps. The average values from data across the spectrum are given in Table 1.

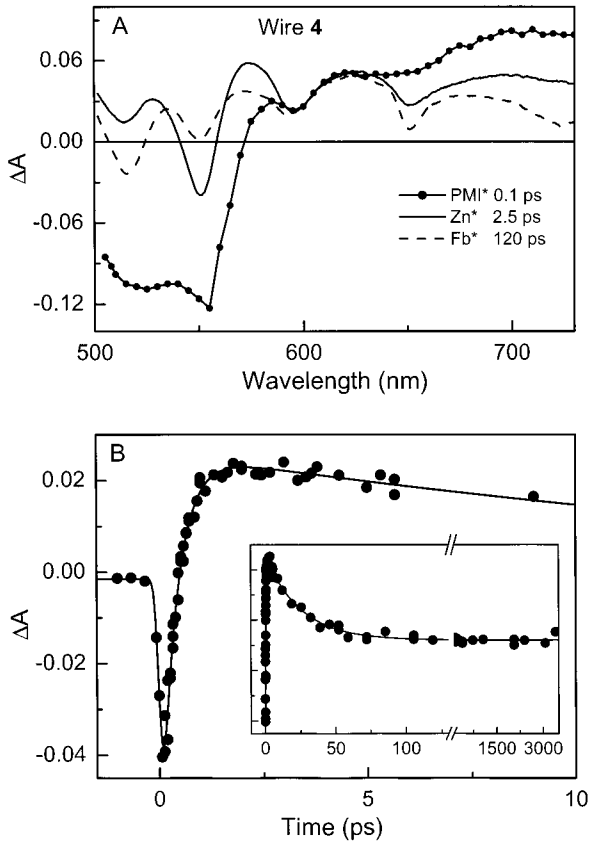

Figure 5. Time-resolved absorption data for wire **4** analogous to those described for wire **2** in Figure 3. The dual-exponential fit to the kinetic trace at 515 nm in B, with the full time window of the measurement in the inset, gives time constants of 0.4 and 24 ps. The average values from data across the spectrum are given in Table 1.

measured for **3** at some wavelengths, and used in obtaining the average Zn* lifetime, may be lengthened somewhat due to convolution with the PMI* decay time. The PMI* lifetime is found to be 5.2 ± 0.8 ps in **3**, as can be seen from the kinetic trace at 630 nm (Figure 4B, inset), which is dominated by decay of the pronounced PMI* excited-state absorption band (Figure 4A). This PMI* lifetime in short wire **3** is the same within experimental uncertainty as that in long wire **2** (Table 1), which is consistent with the fact that the two arrays have the same connectivity between the perylene and adjacent Zn porphyrin (Chart 1).

Transient optical data for wire **4** are shown in Figure 5. The use of a phenylethyne versus diarylethyne linker and attachment at the perylene C9 position versus imide nitrogen in **4** versus **3** has substantial consequences on the transient absorption spectra and kinetics associated with the initial stage of the energy flow. One of the most notable differences is that the pronounced PMI* excited-state absorption band at 635 nm in **4** is substantially broadened, diminished in peak amplitude, and shifted to longer wavelengths compared to the situation in **3** (and **2**, **PMI-aep-Fb**, and **PMI-2**) (compare the 0.1 ps spectrum in Figure 5 with those in Figures 2−4). This difference in excited-state absorption characteristics parallels the broadened and red shifted PMI ground-state absorption features in **4** relative to the other PMI-containing arrays, as described above (see Figure 1D versus Figure 1B,H). Furthermore, the measured PMI* lifetime of ∼0.4 ps in **4** is so short and convolved with the instrument response that a conservative upper limit of ≤0.4 ps is reported. This value is at least 10-fold shorter than the value of ∼5 ps in **3** (and **2** and **PMI-aep-Zn**). This difference can be seen from the initial stage of the time profile reflecting the decay of the PMI* bleaching and formation of the Zn* absorption at 515 nm in Figures 4B and 5B (main traces). We have seen the same effects on the PMI* excited-state absorption characteristics and decay time in our previous study of **PMI-ep-Zn**, which has the same ep linker to the Zn porphyrin and connection to the perylene C9 position employed in wire **4** (Charts 1 and 3).[17] Thus, the spectral properties of the excited input unit and its ultrafast decay by energy transfer to the Zn porphyrin in **4** were anticipated on the basis of studies of the appropriate dyad. Similarly, the subsequent Zn* transient difference spectrum, the 26 ± 3 ps Zn* lifetime (dominated by energy transfer to the Fb porphyrin), the consequent Fb* spectrum, and the long (∼13 ns) Fb* decay in **4** (Figure 5 and Table 1) are basically the same as in wires **2** and **3** studied here and dyads **PMI-ep-Zn** and **ZnFbU** studied previously.[6,17,33,34] This latter behavior derives from the same connectivity between the Zn porphyrin and Fb porphyrin output unit in these arrays.

Analogous studies were conducted on the original long wire **1**, which differs from **2** in the BDPY versus PMI input units and the adjacent aryl ring in the linker (Chart 1). Indeed, the results on **1** differ from those described

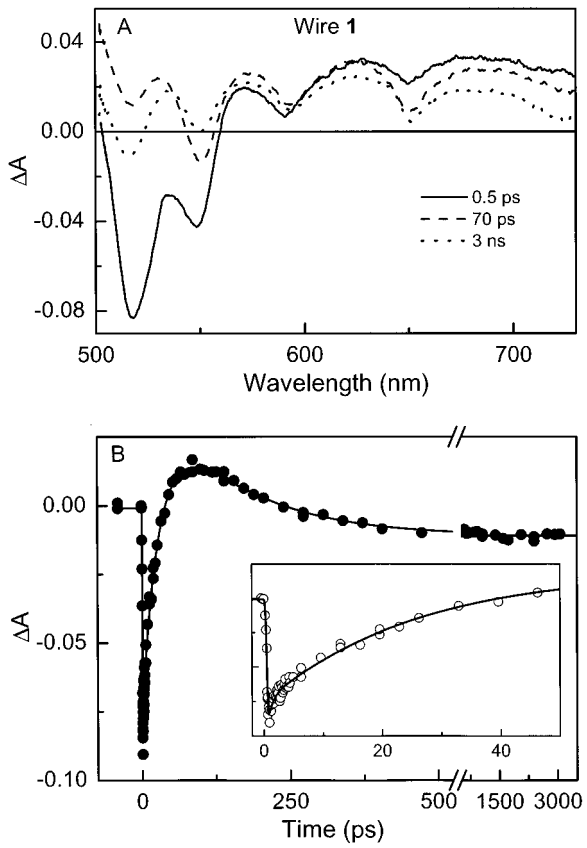

Figure 6. Time-resolved absorption data for wire **1** analogous to those described for wire **2** in Figure 3. The dual-exponential fit to the kinetic trace at 515 nm in B, with the full time window of the measurement in the inset, gives time constants of 25 and 1 ps (with relative amplitudes 85:15 for BDPY* decay) and 170 ps (Zn* decay). The average values from data across the spectrum are given in Table 1.

above for **2** primarily in the spectral changes and kinetics at early times associated with decay of the BDPY* versus PMI* (Figures 2 and 6 and Table 1). In addition to the spectral differences at early times associated with the respective excited input units, the essentially single-exponential PMI* decay in **2** ($\tau = 5.3$ ps) is replaced in **1** with a dual exponential decay dominated (80%) by a slower component with a time constant of 33 ps and a faster component with $\tau = 1.7$ ps. These differences are expected based on studies of the respective dyads (Table 1).[7,18]

Energy-Transfer Rates and Efficiencies. The time-resolved optical data described above and summarized in Table 1 can be used to obtain the energy-transfer rates and efficiencies in the wires using standard equations and assumptions. These methods have been described in detail previously[6,7,15,33] and are summarized in the Supporting Information along with those for the analysis of the companion static emission data described above. The energy-transfer rate constant and yield for a given stage in each wire are given by the expressions $k_{trans} = (1/\tau - 1/\tau^m)$ and $\Phi_{trans} = k_{trans}\tau = 1 - \tau/\tau^m$, where τ is the excited-state lifetime of a particular energy-transfer donor component in the wire and τ^m is the lifetime of the corresponding reference monomer (in which energy transfer is not possible). The overall efficiency for end-to-end transfer in the wire is the product of those for the respective stages.

Using these expressions and the lifetimes in Table 1, the rate constants for energy transfer from the excited input unit (BPDY* or PMI*) to the adjacent Zn porphyrin are determined to be k_{trans} (input → Zn) = (26 ps)$^{-1}$, (5.3 ps)$^{-1}$, (5.2 ps)$^{-1}$, and ≥(0.4 ps)$^{-1}$ for wires **1**−**4**, respectively. (For **1**, the time constant of the longer-lived BDPY* component was used.) A similar calculation gives an energy-transfer efficiency for this initial step of Φ_{trans} (input → Zn) = 95% for wire **1** and >99% for wires **2**−**4**. Energy-transfer rate constants of (17 ps)$^{-1}$, (4.2 ps)$^{-1}$, and ≥(0.4 ps)$^{-1}$ and quantum efficiencies of 94%, 99%, and 99% are obtained for dyads **BDPY-Zn**,[7] **PMI-aep-Zn**,[18] and **PMI-ep-Zn**[17] from the appropriate lifetimes in Table 1. The values for **BDPY-Zn** and **1** are in reasonable accord given the difficulties associated with the dual-exponential character of the BDPY* decay. The values for **PMI-ep-Zn** and **4** coincide, as expected given the identical structural characteristics in the dyads and input sections of these wires. The rate constant of (4.2 ps)$^{-1}$ obtained from the lifetime data[18] for **PMI-aep-Zn** is about 20% greater than the values for wires **2** and **3**. This difference is attributed to the fact that the dyad has steric hindrance only on the aryl ring of the linker attached to the perylene input unit, whereas the two wires have steric hindrance on the aryl ring attached to the Zn porphyrin as well (Charts 1 and 3). In this regard, we have shown previously that steric hindrance on each aryl ring of the linker slows (by about 2-fold) energy transfer between porphyrins due to reduced linker-porphyrin orbital overlap.[33]

Similar calculations reveal that energy transfer from the single Zn porphyrin to the Fb porphyrin output unit in wires **3** and **4** occurs with rate constants k_{trans} (Zn → Fb) = (28 ps)$^{-1}$ and (26 ps)$^{-1}$ and efficiencies Φ_{trans} (Zn → Fb) = 99%. These values are basically the same as those obtained for dyad **ZnFbU** (k_{trans} (Zn → Fb) = (24 ps)$^{-1}$ and Φ_{trans} (Zn → Fb) = 99%),[6,33] which represents the output dyad section of **3** and **4**. When combined with the >99% quantum efficiencies for energy transfer from the perylene input unit to the adjacent Zn porphyrin, the above values show that the end-to-end energy-transfer efficiency is 99% in wires **3** and **4**.

The output stage of each of the long wires **1** and **2** consists of the same diphenylethyne-linked Zn and Fb porphyrins that comprise the output units of wires **3** and **4** and the dyad **ZnFbU** (Chart 4). Accordingly, it is expected that energy transfer to the terminal Fb porphyrin in **1** and **2** from its adjacent Zn porphyrin will occur with the same rate constant of ∼(25 ps)$^{-1}$ described above for **3**, **4**, and **ZnFbU**. However, long wires **1** and **2** each also contains two additional Zn porphyrin transmission elements through which the energy must flow from the BDPY or perylene input unit, respectively. Given that the three Zn porphyrins in either **1** or **2** have approximately equal excited-state energies, reversible energy transfer can occur between these transmission elements in route from the input unit to the Fb porphyrin output unit (or if one of the Zn porphyrins is excited directly by photon absorption). Additionally, although energy transfer to the terminal Fb porphyrin unit in **1** and **2** is expected to occur primarily (and with the fastest rate) from its adjacent Zn porphyrin, our work on other arrays indicates that transfer to the Fb porphyrin likely also occurs from distant Zn porphyrins by superexchange mediated by the intervening Zn porphyrin(s), and with rate constant that is a modest fraction of that for adjacent

chromophores.[7,41] Given these considerations, it is evident that the observed Zn* decay for either wire **1** or **2** represents an effective excited-state lifetime of the three Zn porphyrin transmission elements that incorporates the reversible transfers between these units plus the direct and superexchange-assisted energy transfers to the Fb porphyrin. Similar considerations apply to branched and dendrimeric architectures comprised of up to 21 porphyrins that we have recently prepared and studied.[9]

The effective Zn* lifetime for long wire **1** or **2** can be used to obtain the effective rate constant and the quantum efficiency for energy transfer from the trimeric Zn porphyrin transmission chain to the Fb porphyrin output unit using calculations similar to those described above for short wires **3** and **4**. The measured effective Zn* lifetimes are $\tau = 160 \pm 30$ ps for **1** and 170 ± 30 ps for **2**, compared with the anticipated reference value (in the absence of energy transfer) of $\tau^m = 2.4$ ns in both wires (Table 1). These data afford k_{trans} ($Zn_3 \rightarrow Fb$) = $(171\ ps)^{-1}$ and Φ_{trans} ($Zn_3 \rightarrow Fb$) = 93% for wire **1** and k_{trans} ($Zn_3 \rightarrow Fb$) = $(183\ ps)^{-1}$ and Φ_{trans} ($Zn_3 \rightarrow Fb$) = 92% for wire **2**. Multiplying this value by the 95% or >99% value for efficiency for energy flow from the BDPY or PMI input unit to the adjacent Zn porphyrin gives an overall end-to-end efficiency of 88% in wire **1** and 92% in wire **2**. These estimates can be combined with those from the analyses of the static emission data described above, taking into account the assumptions and uncertainties associated with each assay. The conclusion is that the end-to-end energy-transfer efficiency is 81 ± 9% in wire **1** and 86 ± 7% in wire **2**. The overall energy-transfer rate constants are obtained by summing those of the individual stages; these are found to be $(190\ ps)^{-1}$ for wire **1** and $(175\ ps)^{-1}$ for wire **2**.

Conclusions

Using a modular building block approach, we have constructed four porphyrin-based, weakly coupled molecular photonic wires. The wires utilized either BDPY or perylene dyes as input units and contain a varying number of Zn porphyrin "transmission elements" between the input and Fb porphyrin output unit. The perylene dye was found to be superior to BDPY as the input unit because the former exhibits a monophasic excited-state lifetime and nearly unit quantum yield of fluorescence. Regardless, each of the four molecular wires exhibits rapid, efficient through-bond energy transfer that ultimately delivers photonic energy from the input to the output unit. The overall energy-transfer rate constants and quantum efficiencies are greater for the "short" wires than the "long" wires: short wire **3**, $(33\ ps)^{-1}$ and >99%; short wire **4**, $(26\ ps)^{-1}$ and >99%; long wire **1**, $(190\ ps)^{-1}$ and 81%; long wire **2**, $(175\ ps)^{-1}$ and 86%. The somewhat decreased rate and efficiency of energy transfer in the original, long BDPY-based wire (**1**) is due mainly to "losses" among the transmission elements, with some loss at the initial stage involving the input unit and the first transmission element. The modestly decreased rate and efficiency in the new, long PMI-based wire (**2**) is due exclusively to losses among the transmission elements with virtually no loss at the input stage. In all the wires, once energy has arrived at the output unit, no diminution in energy available for emission or subsequent transmission to (future) additional stages is incurred via interactions with other components in the arrays.

The results reported herein indicate that the design and implementation of the new PMI-based wires eliminate some of the deficiencies in the original BDPY-based construct. Most notably, complexities associated with the prominent dual-exponential decay of the input unit and energy loss in transfer to the first transmission element are basically absent with a PMI input unit. Accordingly, any additional improvements in energy-transfer efficiency will require attenuation in the "transmission loss." To address this issue, we are investigating a number of architectures that contain multiple Zn porphyrins (as well as other components) in order to deduce the energy-transfer time between Zn porphyrins. These studies are also relevant to issues pertaining to isoenergetic energy transfer between identical chromophores in very large synthetic light-harvesting arrays[9] and natural photosynthetic light-harvesting systems.[2] In parallel, we are pursuing two strategies involving modifications to the linkages and elements in the transmission chains. In one approach, Zn porphyrins identical to those used in **1** and **2** but joined by *p*-phenylene (rather than diarylethyne linkers) are being employed. Our previous studies on *p*-phenylene-linked Zn and Fb porphyrins showed that the energy-transfer rate is increased to $(3.5\ ps)^{-1}$ from $(24\ ps)^{-1}$ in the 4,4′-diphenylethyne-linked analogue, while retaining a weakly coupled system. We expect similar enhancements (and concomitant diminution of energy losses) for transfer among Zn porphyrins in *p*-phenylene-linked transmission chains. In the second approach, we are exploring alternative transmission-chain chromophores such as chlorins that have stronger visible-region transitions. These new components are expected to give enhanced rates of energy transfer via increased through-space contributions, as well as enhanced light-harvesting properties for other applications.

Collectively, the studies reported herein emphasize that relatively weak electronic coupling can afford rapid excited-state energy transfer. Weakly coupled systems are attractive and of significant practical utility. In particular, architectures of increasing complexity can be synthesized in a rational manner to have desired properties based on fundamental knowledge of the component subunits. This approach is possible because the inherent electronic properties of the ground and lowest excited states of the components are essentially retained in the more complex arrays.

Experimental Section

General Methods. ^{1}H NMR spectra (300 MHz) were recorded in $CDCl_3$ unless noted otherwise. Absorption spectra and fluorescence spectra were routinely collected in toluene for sample characterization. Porphyrins were analyzed by LD-MS in the absence of a matrix[42] or using the matrix 1,4-bis-(5-phenyloxazol-2-yl)benzene (POPOP). 4-Iodobenzaldehyde was obtained from Karl Industries, Ltd.

Optical Spectroscopy. The electronic absorption spectra reported in Figure 1 were obtained using a Cary 100 spec-

(41) (a) Lammi, R. K.; Ambroise, A.; Balasubramanian, T.; Wagner, R. W.; Bocian, D. F.; Holten, D.; Lindsey, J. S. *J. Am. Chem. Soc.* **2000**, *122*, 7579−7591. (b) Lammi, R. K.; Ambroise, A.; Wagner, R. W.; Diers, J. R.; Bocian, D. F.; Holten, D.; Lindsey, J. S. *Chem. Phys. Lett.* **2001**, *341*, 35−44.

(42) (a) Fenyo, D.; Chait, B. T.; Johnson, T. E.; Lindsey, J. S. *J. Porphyrins Phthalocyanines* **1997**, *1*, 93−99. (b) Srinivasan, N.; Haney, C. A.; Lindsey, J. S.; Zhang, W.; Chait, B. T. *J. Porphyrins Phthalocyanines* **1999**, *3*, 283−291.

trometer using 0.25 nm data intervals, a scan speed of 600 nm/min and a bandwidth of 1 nm toluene. The emission spectra in Figure 1 were measured using a Spex Tau2 spectrofluorimeter with slit widths of 5 nm for excitation and 2 nm for detection. Nondegassed samples ($\leq 1 \times 10^{-5}$ M) in toluene at room temperature were employed for both the absorption and emission experiments. Further details on the protocols for specific emission measurements such as determination of fluorescence yields are given in the Supporting Information. Transient absorption data were obtained at room temperature as described elsewhere.[43] Samples (~0.1−0.2 mM in toluene) in 2-mm path length cuvettes were excited at 10 Hz with 130-fs pump pulses (5−10 μJ at 400−450 nm, 25−35 μJ at 480−590 nm) and probed with white light pulses of comparable duration.

Chromatography. Adsorption column chromatography was performed using flash silica. Preparative scale size exclusion chromatography (SEC) was performed using BioRad Bio-Beads SX-1 in a glass column (5 × 75 cm) packed with either HPLC-grade THF or toluene. The chromatography was performed with gravity flow (~4 mL/min). A typical separation required ~3 h. Following purification, the SEC column was washed with solvent. Unlike adsorption columns, the SEC columns can be used repeatedly, although with continued use for porphyrin separations the columns become uniformly slightly pink-brown.

Analytical scale SEC was performed to assess the purity of the arrays and to monitor the reactions using a 1000 Å column (260 × 12 mm, 5 μm) eluting with THF (flow rate = 0.8 mL/min) at 40 °C. Reactions were monitored by removing aliquots from the reaction mixture and diluting with THF prior to analysis by SEC.

Solvents. CH_2Cl_2 (reagent grade) and $CHCl_3$ (A.C.S. grade; 0.75% ethanol as stabilizer) were used as received. Toluene (A.C.S. grade) and triethylamine were distilled from CaH_2. THF and toluene (HPLC grade) were used for preparative SEC. Other solvents were used as received.

Noncommercial Compounds. The following compounds were prepared as described in the literature: porphyrins **FbU′**[31] and **5**,[12] boron-dipyrrin dye **9**,[13] perylene-monoimide dyes **10**[18] and **11**,[23] and dyad **12**.[30]

Dyad 6. To samples of **FbU′** (300 mg, 0.392 mmol), **5** (396 mg, 0.391 mmol), $Pd_2(dba)_3$ (54 mg, 0.060 mmol), and P(*o*-tol)$_3$ (147 mg, 0.480 mmol) was added a degassed solution of toluene/triethylamine (159 mL, 5:1). The flask was immersed in an oil bath and stirred at 35 °C. Samples were removed periodically (~1 h intervals) for analysis by SEC. The reaction was judged to be complete after 3 h. The reaction mixture was concentrated to dryness. The resulting residue was dissolved in a minimum amount of CH_2Cl_2 and loaded on a silica column (4 × 25 cm). Elution with CH_2Cl_2/hexanes (1:1) afforded P(*o*-tol)$_3$ followed by the porphyrin species (~600 mL of eluant), while the Pd species remained bound to the top of the column. The mixture of porphyrins was then concentrated to dryness, dissolved in a minimum amount of THF, and loaded on a preparative SEC column (5 × 75 cm). Gravity elution (650 mL of THF) afforded three bands (in order of elution): higher molecular weight material, desired dyad, and monomeric porphyrin. The dyad fraction (tailing with higher molecular weight material) was collected and concentrated to dryness, dissolved in a minimum amount of THF and loaded on the preparative SEC column. Gravity elution afforded the dyad as a distinct band. The dyad fraction was concentrated, dissolved in a minimum amount of CH_2Cl_2 and chromatographed [5 × 20 cm, silica, CH_2Cl_2/hexanes (1:1)]. Concentration of the dyad fraction afforded a purple solid (340 mg, 52%): ^{1}H NMR δ −2.53 (brs, 2H), 0.37 (s, 9H), 1.87 (m, 36H), 2.64 (m, 15H), 7.28 (m, 10H), 7.63 (s, 2H), 8.06 (d, J = 7.8 Hz, 4H), 8.29 (m, 4H), 8.65−8.95 (m, 16H); LD-MS obsd 1647.4; calcd exact mass 1646.7 ($C_{112}H_{98}N_8SiZn$); λ_{abs} 426, 516, 550, 592, 650 nm; λ_{em} (λ_{ex} = 550 nm) 651, 720 nm. A second reaction (0.26 mmol) afforded 240 mg (56%); a third reaction (0.13 mmol) afforded 98 mg (46%).

Ethynyl-dyad 6′. A solution of dyad **6** (95 mg, 0.060 mmol) in THF (20 mL) was treated with TBAF on silica gel (120 mg, 1.0−1.5 mmol F^-/g of resin). The reaction mixture was stirred at room temperature for 3 h. The reaction mixture was evaporated to dryness and dissolved in 200 mL of CH_2Cl_2. The organic layer was washed with 5% aqueous $NaHCO_3$ and water. The organic layer was dried (Na_2SO_4), concentrated, and chromatographed [silica, CH_2Cl_2/hexanes (1:1)] affording a purple solid (88 mg, 92%): ^{1}H NMR δ −2.53 (brs, 2H), 1.87 (m, 36H), 2.64 (m, 15H), 3.25 (s, 1H), 7.28 (m, 10H), 7.64 (s, 2H), 8.06 (d, J = 8.1 Hz, 4H), 8.29 (m, 4H), 8.65−8.95 (m, 16H); LD-MS obsd 1575.40; calcd exact mass 1574.66 ($C_{109}H_{90}N_8Zn$); λ_{abs} 426, 515, 550, 592, 650 nm; λ_{em} (λ_{ex} = 550 nm) 651, 721 nm. A similar reaction (0.33 mmol, 10 mL toluene and 60 mL THF) gave 506 mg (96%).

Triad 7. Samples of **6′** (90 mg, 0.057 mmol) and **5** (58 mg, 0.057 mmol) were coupled using $Pd_2(dba)_3$ (8.0 mg, 8.5 μmol) and P(*o*-tol)$_3$ (21 mg, 0.068 mmol) in toluene/triethylamine [23 mL (5:1)] at 35 °C for 3 h. The reaction mixture was concentrated to dryness. The crude reaction mixture was dissolved in toluene and warmed in a hot water bath at 45 °C for 3 min to achieve complete dissolution prior to chromatography [silica, CH_2Cl_2/hexanes (1:1)]. The resulting mixture of porphyrins was concentrated to dryness, dissolved in a minimum amount of toluene and loaded on a preparative SEC column. Gravity elution afforded four bands (in order of elution): higher molecular weight material, desired triad, dyad and monomeric porphyrins. The triad fraction was concentrated to dryness, dissolved in a minimum amount of toluene and loaded on a preparative SEC column (toluene) to remove the small amount of higher molecular weight material tailing with the triad. The triad fraction was concentrated, dissolved in a minimum amount of toluene and chromatographed [silica, toluene/hexanes (2:1)], affording a purple solid (60 mg, 42%): ^{1}H NMR δ −2.53 (brs, 2H), 0.37 (s, 9H), 1.87 (m, 54H), 2.64 (m, 21H), 7.28 (m, 14H), 7.63 (s, 2H), 7.84 (s, 2H), 8.07 (m, 6H), 8.30 (m, 6H), 8.66−8.98 (m, 24H); LD-MS obsd 2455.62; calcd exact mass 2456.97 ($C_{166}H_{140}N_{12}SiZn_2$); λ_{abs} 423, 430, 515, 551, 591, 650 nm; λ_{em} (λ_{ex} = 550 nm) 651, 721 nm. A similar reaction (0.14 mmol) gave 161 mg (46%).

Ethynyl-Triad 7′. A solution of **7** (211 mg, 0.0857 mmol) in toluene/THF [50 mL (4:1)] was treated with TBAF on silica gel (180 mg, 1.0−1.5 mmol F^-/g of resin) with stirring at room temperature for 3 h. The reaction mixture was evaporated to dryness and dissolved in toluene, washed with 5% aq $NaHCO_3$ followed by water, and dried (Na_2SO_4). The reaction mixture was concentrated to dryness. The crude reaction mixture was dissolved in toluene and warmed in a hot water bath at 45 °C for 3 min to achieve complete dissolution prior to chromatography [silica, toluene/hexanes (4:1)], affording a purple solid (198 mg, 97%): ^{1}H NMR δ −2.53 (brs, 2H), 1.88 (m, 54H), 2.65 (m, 21H), 3.26 (s, 1H), 7.28 (m, 14H), 7.64 (s, 2H), 7.84 (s, 2H), 8.06 (m, 6H), 8.30 (m, 6H), 8.67−8.98 (m, 24H); LD-MS (POPOP) obsd 2388.76; calcd exact mass 2384.93 ($C_{163}H_{132}N_{12}Zn_2$); λ_{abs} 423, 430, 515, 551, 591, 650 nm; λ_{em} (λ_{ex} = 550 nm) 651, 721 nm. A similar reaction (175 mg, 0.070 mmol) gave 150 mg (90%).

Tetrad 8. Samples of **7′** (198 mg, 0.0828 mmol) and **5** (84 mg, 0.083 mmol) were coupled using $Pd_2(dba)_3$ (12 mg, 0.013 mmol) and P(*o*-tol)$_3$ (30 mg, 0.10 mmol) in toluene/triethylamine (33 mL, 5:1) at 35 °C for 3 h. Standard workup (as for **7**) afforded a purple solid (95 mg, 35%): ^{1}H NMR δ −2.53 (brs, 2H), 0.38 (s, 9H), 1.87 (m, 72H), 2.65 (m, 27H), 7.30 (m, 18H), 7.63 (s, 2H), 7.84 (s, 4H), 8.06 (m, 8H), 8.31 (m, 8H), 8.66−8.98 (m, 32H); LD-MS obsd 3269.09; calcd exact mass 3267.24 ($C_{220}H_{182}N_{16}SiZn_3$); λ_{abs} 423, 432, 515, 551, 591, 650 nm; λ_{em} (λ_{ex} = 550 nm) 651, 721 nm. A similar reaction (0.054 mmol) gave 74 mg (43%).

Ethynyl-Tetrad 8′. A solution of **8** (74 mg, 0.023 mmol) in toluene/THF [20 mL (4:1)] was treated with TBAF on silica gel (46 mg, 1.0−1.5 mmol F^-/g of resin) with stirring at room

(43) (a) Kirmaier, C.; Holten, D. *Biochemistry* **1991**, *30*, 609−613. (b) Yang, S. I.; Lammi, R. K.; Seth, J.; Riggs, J. A.; Arai, T.; Kim, D.; Bocian, D. F.; Holten, D.; Lindsey, J. S. *J. Phys. Chem. B* **1998**, *102*, 9426−9436. (c) Yang, S. I.; Li, J.; Cho, H. S.; Kim, D.; Bocian, D. F.; Holten, D.; Lindsey, J. S. *J. Mater. Chem.* **2000**, *10*, 283−296.

temperature for 3 h. Standard workup (as for **7′**) afforded a purple solid (66 mg, 91%): ^{1}H NMR δ −2.53 (brs, 2H), 1.88 (m, 72H), 2.65 (m, 27H), 3.25 (s, 1H), 7.28 (m, 18H), 7.64 (s, 2H), 7.84 (s, 4H), 8.07 (m, 8H), 8.31 (m, 8H), 8.66−8.99 (m, 32H); LD-MS obsd 3196.19; calcd exact mass 3195.20 ($C_{217}H_{174}N_{16}Zn_3$); λ_{abs} 423, 432, 515, 551, 591, 650 nm; λ_{em} (λ_{ex} = 550 nm) 651, 720 nm. A similar reaction (0.070 mmol) gave 150 mg (90%).

Molecular Wire 1. Samples of **8′** (18 mg, 5.6 μmol) and BDPY **9** (3.0 mg, 7.1 μmol) were coupled using $Pd_2(dba)_3$ (1.0 mg, 0.84 μmol) and P(*o*-tol)$_3$ (2.0 mg, 6.7 μmol) in toluene/triethylamine [2.5 mL (5:1)] at 35 °C for 2 h. Standard workup (as for **7**) with silica chromatography [toluene/hexanes (4:1)] afforded a mixture of porphyrins. The mixture of porphyrins was then concentrated to dryness, dissolved in a minimum amount of toluene with warming, and loaded on a preparative SEC column (toluene). The higher molecular weight material eluted as the first band followed by the title compound (along with unreacted tetrad) as the second band. Further chromatography [silica, toluene/hexanes (4:1)] afforded the unreacted tetrad as the first band followed by the title compound, affording a purple solid (14 mg, 71%): ^{1}H NMR δ −2.53 (brs, 2H), 1.88 (m, 72H), 2.65 (m, 33H), 6.33 (d, J = 3.6 Hz, 2H), 6.81 (d, J = 4.0 Hz, 2H), 7.30 (m, 18H), 7.58 (d, J = 7.6 Hz, 2H), 7.72 (s, 2H), 7.78 (d, J = 7.6 Hz, 2H), 7.84 (s, 4H), 8.07 (m, 8H), 8.31 (m, 8H), 8.66−8.98 (m, 32H); LD-MS obsd 3489.31; calcd exact mass 3489.31 ($C_{234}H_{187}BF_2N_{18}Zn_3$); λ_{abs} 423, 432, 516, 551, 591, 650 nm; λ_{em} (λ_{ex} = 550 nm) 651, 721 nm.

Molecular Wire 2. Samples of **8′** (50 mg, 0.016 mmol) and **10** (9.0 mg, 16 μmol) were coupled using $Pd_2(dba)_3$ (2.0 mg, 2.4 μmol) and P(*o*-tol)$_3$ (6.0 mg, 0.020 μmol) in toluene/triethylamine [6 mL (5:1)] at 40 °C for 2 h. The reaction mixture was rotary evaporated to dryness. The resulting residue was dissolved in a minimum amount of $CHCl_3$ and chromatographed [silica (5 × 10 cm), $CHCl_3$/hexanes (4:1)]. The resulting mixture of porphyrins was then concentrated to dryness, dissolved in a minimum amount of toluene and warmed in a water bath to achieve complete dissolution, then loaded on a preparative SEC column. The higher molecular weight material eluted as the first band followed by the desired compound and unreacted tetrad as the second band. Further chromatography [silica, $CHCl_3$/hexanes (4:1)] afforded the unreacted tetrad as the first band followed by the title compound, affording a purple solid (10 mg, 24%): LD-MS obsd 3674.31; calcd exact mass 3670.40 ($C_{251}H_{199}N_{17}O_2Zn_3$); λ_{abs} 423, 432, 482, 513, 551, 591, 650 nm; λ_{em} (λ_{ex} = 480 nm) 720, 651 nm.

Molecular Wire 3. Samples of **6′** (20 mg, 0.013 mmol) and **10** (10 mg, 16 μmol) were coupled using $Pd_2(dba)_3$ (2.0 mg, 2.4 μmol) and P(*o*-tol)$_3$ (5.0 mg, 0.016 μmol) in toluene/triethylamine [5 mL (5:1)] at 40 °C for 3 h. The reaction mixture was rotary evaporated to dryness. The resulting residue was dissolved in a minimum amount of CH_2Cl_2 and chromatographed [silica (5 × 10 cm), CH_2Cl_2/hexanes (4:1)]. The resulting mixture of porphyrins was then concentrated to dryness, dissolved in a minimum amount of THF and loaded on a preparative SEC column. The higher molecular weight material eluted as the first band followed by the title compound as the second band. The latter was chromatographed [silica, CH_2Cl_2/hexanes (4:1)], affording a purple solid (10 mg, 38%): ^{1}H NMR δ −2.52 (brs, 2H), 1.26 and 1.28 (s, 12H), 1.90 (m, 36H), 2.65 (m, 15H), 2.81 (m, 2H), 7.25 (m, 14H), 7.69 (m, 5H), 7.96 (AA′BB′, 4H), 8.07 (AA′BB′, 4H), 8.31 (t, J = 10.4 Hz, 2H), 8.52 (m, 3H), 8.65−8.97 (m, 16H); LD-MS obsd 2051.69; calcd exact mass 2053.85 ($C_{143}H_{115}N_9O_2Zn$); λ_{abs} 427, 482, 513, 550, 591, 650 nm; λ_{em} (λ_{ex} = 480 nm) 720, 651 nm.

Molecular Wire 4. Samples of **11** (20 mg, 0.034 mmol) and **12** (50 mg, 0.032 mmol) were coupled using $Pd_2(dba)_3$ (5.0 mg, 5.5 μmol) and P(*o*-tol)$_3$ (12 mg, 0.039 μmol) in toluene/triethylamine (13 mL, 5:1) at 60 °C for 3 h. Standard workup (as for **3**) including silica chromatography [CH_2Cl_2/hexanes (1:1)], preparative SEC, and silica chromatography [CH_2Cl_2/hexanes (1:1)] afforded a purple solid (39 mg, 59%): ^{1}H NMR δ −2.52 (brs, 2H), 1.33 and 1.35 (s, 18H), 1.88 (m, 30H), 2.64 (m, 15H), 7.06 (d, J = 2.0 Hz, 1H), 7.28 (m, 10H), 7.47 (dd, J = 2.4 Hz, 6.4 Hz, 1H), 7.61 (d, J = 8.4 Hz, 1H), 7.86 (t, J = 8.0 Hz, 2 H), 8.05 (m, 8H), 8.32 (m, 7H), 8.53 (t, J = 8.4 Hz, 3H), 8.59 (d, J = 8.0 Hz, 1H), 8.65 (s, 3H), 8.72 (m, 4H), 8.84 (m, 5H), 8.95 (m, 4H); LD-MS (POPOP) obsd 2051.95; calcd exact mass 2053.85 ($C_{143}H_{115}N_9O_2Zn$); λ_{abs} 427, 514, 549, 594, 650 nm; λ_{em} (λ_{ex} = 490 nm) 651, 721 nm.

Acknowledgment. This research was supported by a grant from the Division of Chemical Sciences, Office of Basic Energy Sciences, Office of Energy Research, Department of Energy (to J.S.L.), and grants from the National Institutes of Health (GM 34685 to D.H. and GM 36243 to D.F.B.). Mass spectra were obtained at the Mass Spectrometry Laboratory for Biotechnology at North Carolina State University. Partial funding for the NCSU Facility was obtained from the North Carolina Biotechnology Center and the NSF.

Supporting Information Available: A summary of the synthesis of **1**; a description of static fluorescence measurements and the derivation of energy-transfer yields therefrom; methods and results from nine energy-transfer simulations for **1**−**3** using PhotochemCAD; and ^{1}H NMR, LD-MS (or MALDI-MS), SEC chromatograms, absorption spectra, and fluorescence spectra of selected compounds. This material is available free of charge via the Internet at http://pubs.acs.org.

JO025561I